To the Graduate Council:

I am submitting herewith a thesis written by Isaac W. Diggs entitled "Curvature and Its Effects on Heat Transfer with Thermal Radiation in the Free Jet Boundary." I recommend that it be accepted in partial fulfillment of the requirements for the degree of Master of Science, with a major in Engineering Science.

K. H. Kim

K. H. Kim, Major Professor

We have read this thesis and recommend its acceptance:

J H Forrester

Wayman P. Scott

Accepted for the Council:

L Evans Roth

Vice Chancellor
Graduate Studies and Research

CURVATURE AND ITS EFFECTS ON HEAT TRANSFER WITH THERMAL RADIATION IN THE FREE JET BOUNDARY

A Thesis
Presented for the
Master of Science
Degree
The University of Tennessee, Knoxville

Isaac W. Diggs
December 1980

DEDICATION

This work is dedicated

to my wife and children

who demonstrated extreme patience and understanding

throughout the course of my studies.

ACKNOWLEDGMENTS

My deepest appreciation and thanks go to Dr. K. H. Kim, who acted as my thesis advisor and who provided many helpful suggestions. He was able to provide me with direction and answers to many questions which no doubt would have left me far short of my goal at this point had they gone unanswered. Thanks also to Messrs. Ed Denny and Bob Stephenson of the Union Carbide Corporation, Nuclear Division, whose logistical support in the form of computing facilities and programming hints were most essential in making the work go more smoothly.

A special thanks is in order to my boss, Ted Lankford. His understanding and willingness to do whatever he could to make things easier for me during the course of my studies made the task of integrating the roles of student and employee much easier.

ABSTRACT

This investigation was conducted to determine the effects of curvature on the thermal boundary layer in curved jet-type flow fields. Particular interest was directed to examining these effects in the presence of thermal radiation. The investigation was initiated by first determining a set of transformation variables for the boundary layer equations which would allow their reduction to ordinary differential form. Solution of these equations based on assumptions of local similarity in the flow field provided the mechanism through which the effects of curvature could be studied.

The chief applications involved in solution of the problem included the principles and theory of fluid mechanics and heat transfer as related to incompressible, viscous flows where properties such as viscosity and thermal conductivity were assumed invariant. Techniques of numerical analysis utilized to generate the solution sets for various values of the curvature parameter, R, employed the Runge-Kutta algorithm with Gill Coefficients. This algorithm was employed in a program designed to generate solutions based on automatic corrections to initial guesses for starting values given to the slopes of the velocity and temperature profiles. Solution of the momentum equation first provided values for the dimensionless stream function which were needed in

solution of the energy equation. Additionally, analysis of the asymptotic boundary conditions at both extremes of the thermal boundary layer provided the information needed to define a "feasible set" of starting values to be used in conjunction with the stream function to arrive at the required solution for the temperature profile.

The results obtained from the research indicate that the major effect of curvature on the mixing zone in the free jet boundary is alteration of the thermal boundary layer thickness with increasing value of the curvature parameter. This effect was seen to exist both in the presence of, and in the absence of thermal radiation. Calculations were performed for differing values of the conduction-to-radiation parameter, N, which defines the relative degree of radiative versus conductive contribution to the thermal boundary layer. For values of N greater than 1, which coincides with the lessening influence of radiative transfer, the thermal boundary layer was found to grow with increases in the curvature parameter. On the other hand, however, the dominant influence of radiative transfer represented by values of N less than 1 showed a decrease in the thickness of the thermal boundary layer for increasing curvature. Coincident with the change in boundary layer thickness for this situation, a decrease in the value of the temperature along the major streamline accompanied the increase in curvature. These two phenomena, as related to optically thick radiation, can be explained through the fact that optically thick radiation restricts thermal transfers among molecules in the fluid to neighbors in close proximity of one another. Others had established before this study that the velocity profile within the outer confines of the boundary layer changed significantly with curvature. The resultant effect on the motion of the molecules in the flow field in this region would obviously have an effect on the capability for radiative transfers within the flow.

The linearizing technique which was utilized for the first order approximation to the solution of the energy equation provides, at best, some insight into the general behavior of the temperature profile within the thermal boundary layer. The roughness of this approximation is due primarily to the assumption of very small temperature differences across the mixing zone. The accuracy of the results is also affected by the error inherent in adoption of the optically thick approximation for radiative heat flux across the thermal boundary layer. Future studies should concentrate on development of techniques which allow more precise analyses to be conducted. A good point of departure would be one where the nonlinear form of the energy equation is used to more adequately predict the temperature profile in the boundary layer. More exact expressions for the radiative heat flux may also be employed in an effort to gain a better perspective into the problem of completely specifying thermal behavior.

TABLE OF CONTENTS

LIST OF SYMBOLS

A_q	turbulent conductivity constant
A_τ	turbulent viscosity constant
C	eddy viscosity proportionality constant
C_p	specific heat
f	dimensionless stream function
f′	dimensionless velocity function
K	thermal conductivity
l	mixing length
N	conduction-to-radiation parameter
P, $\overline{P}$	pressure, laminar and turbulent mean
P_t	turbulent Prandtl number
Pr	laminar Prandtl number
q_c	conductive heat flux
q_m	heat flux across major streamline
q_r	radiative heat flux
R	curvature
$\mathcal{R}$	similarity curvature parameter
R_e	Reynolds number
T_s, T_∞	temperature, stagnation and freestream
u, $\overline{u}$	x velocity component, laminar and turbulent
U_1	major streamline velocity
U_{max}	freestream velocity
v, $\overline{v}$	y velocity component, laminar and turbulent
z	mixing length proportionality constant
α	thermal diffusivity
β	coefficient of thermal expansion
β_1, β_2	integration constants
γ	integration constant
ε	eddy viscosity
η	similarity transformation independent variable

θ	dimensionless temperature
κ	absorptivity
λ	thermal radiation wavelength
μ	dynamic viscosity
ν	kinematic viscosity
π	eddy conductivity
ρ	density
σ	Stefan-Boltzman constant
τ	shear stress
ψ	similarity transformation stream function
ω	turbulent similarity transformation constant

CHAPTER I

INTRODUCTION

Much effort has been expended in the analysis of problems associated with an understanding of the phenomena occuring in so called free flows. The literature contains many references to investigations by various researchers. Schlichting [1], for example, discusses a number of studies involving the free flows defined as jets and wakes. White [2] also provides some insight into other investigations which have been carried out. Particular interest in this thesis is directed toward the jet boundary, which occurs when two adjacent streams move in the same general direction with different velocities. The velocity discontinuity causes a mixing region to develop along the common boundary of the two streams with the result that movement downstream in the flow will show an increase in the width of the mixing zone. According to Schlichting [1], the first solution to this particular problem was given by Tollmein in 1945. Tollmein's solution involved application of Prandtl's mixing length hypothesis to the problem of momentum transfer in the mixing zone. In the same work, Schlichting also reported very good agreement between a theoretical solution for velocity profiles provided by Goertler, and experimental work performed by Reichardt.

More recently, attention has been given to reattaching flows where a pressure differential across the flow profile causes the stream to curve and attach itself to an adjacent wall. This phenomenon, known as the "Coanda" effect, finds many useful applications in the field of fluidics. Sawyer [3] provides a very interesting analysis of the momentum transfer processes evident in the entrainment of stagnant fluid in a cavity formed by reattachment of a curved two dimensional jet to an adjacent wall. He further expanded this analysis [4] to include variations in curvature of the jet and its effects on fluid entrainment by the moving stream. The results of his analysis indicated that curvature had a significant effect on the rate of fluid entrainment but that the velocity distributions in the jet were not necessarily similarly affected. These experiments, though based on dimensional consideration of a simple flow model for the two dimensional turbulent jet, give some insight into the importance of entrainment in the momentum transfer which takes place in jet boundary-type flows. The theoretical study reported by Williams, Cheng and Kim [5] examined the effects of curvature on the velocity profiles of both the laminar and turbulent flow regimes as associated with the free jet boundary. This study differed from the modeling and experimental study done by Sawyer in that a similarity solution to the boundary layer equations of motion was developed to describe the velocity profiles in the flow. Their results regarding curvature show agreement with the proposition put forth by Murphy [6] concerning the fact that the velocity profile is most affected near the outer edge of the boundary layer (or mixing zone in this case).

The above discussion has established the relative significance of fluid entrainment in the analysis of momentum transfer in free flows. Additionally, the great utility of the Prandtl mixing length hypothesis, especially in the analysis of turbulent free flows, has been widely acknowledged in the literature cited thus far. The question concerning the role of entrainment in heat transfer occurring in free flows, however, must also be examined if the analysis is to be complete. A thorough understanding of the mechanisms of heat transfer is especially important in situations where temperature distributions play a role in the efficiency of an operating system. Consider, for instance, the case where a gas at very high temperature is expelled through a nozzle into a cavity where the ambient temperature is at some different value. Insight into how these temperature differences might affect the resulting flow field would prove to be very useful. If the temperature of the moving fluid is sufficiently high, thermal radiation will be evident in addition to the normal convective transfers expected.

A number of studies have been conducted involving the heat transfer mechanisms in jets and wakes. Schlichting [1] reports on temperature measurements made by Fage and Falkner in 1932 in the wake behind a row of heated bars where they deduced that the temperature profile in such a flow field is wider than the velocity profile. He also provides information on a number of investigations performed by others such as Corrsin and Uberoi, and Hinze and Van der Hegge Zignen. These studies examined temperature distributions in heated circular turbulent jets. One of the more remarkable contributions to the study of heat transfer in free flows, however, was made by Reichardt [7]. He was able to provide an empirical relation, through experimental and theoretical analysis, which linked velocity and temperature distributions through a power law relationship. These works have all contributed to the body of knowledge but are incomplete for application to the situation involving curvature and thermal radiation in a free jet-type flow.

Some further basis for understanding the problem at hand can be gained through examination of contributions to the generalized boundary layer theory made by other researchers. Kestin and Richardson [8] presented a detailed analysis of the theory associated with heat transfer across turbulent boundary layers and, though they primarily treated conditions of forced convection, their fundamental explanations on the nature of thermal boundary layer formation and on the attendant effects of changes in fluid properties provide an excellent point of departure for the study of more complex situations. The work contributed by Viskanta and Grosh [9] examines the effects of thermal radiation on the temperature profiles across the boundary layer of an absorbing and emitting medium by using the Rosseland approximation to the radiation flux vector in the energy equation. They found that use of this approximation is valid when the boundary layer under consideration is optically thick with respect to incident radiation. Others [10, 11] have also examined the effects of thermal radiation in the boundary layer, specifically in high temperature gas flows.

This brief survey of the available literature, both theoretical and experimental, lends itself to a greater appreciation for the fundamental aspects of analysis required in the solution of boundary problems associated with free flows. A void appears to exist, nonetheless, with respect to complete definition of the relationships which may exist among fluid entrainment, momentum transfer, and heat transfer when radiation effects are evident in curved flow fields. The work by Williams, Cheng, and Kim, already cited, relates the aspects of entrainment and momentum transfer in a curved free jet boundary, but the connection is not drawn between these two processes and the temperature distributions present. It is expected that since the rate of entrainment is significantly affected by curvature [3, 4], the heat transfer mechanisms evident in the jet boundary flow will also be similarly affected. The literature surveyed has not indicated a great deal of effort devoted to the study of heat transfer in curved flow fields since 1974. It is the purpose of this thesis to fill the void mentioned above and to provide a measure of continuity to the work which has already been done.

Chapter II will develop the theoretical framework necessary to effectively treat this problem based on assumptions of similarity in the flow field in the free jet boundary. An analysis of the solution and supporting data in Chapter III will be followed by a discussion of conclusions and recommendations in Chapter IV.

CHAPTER II

THEORETICAL DEVELOPMENT

A. Equations of the Boundary Layer

Most investigations involving the analysis of flows in a boundary layer region make use of the so-called boundary layer equations. Due to the nature of formation of the free jet boundary, these equations may be employed here. The equations as generally expressed when two dimensional, incompressible flow with constant properties (viscosity, density, and thermal conductivity) is assumed are [2]:

$$\frac{\partial u}{\partial x} + \frac{\partial v}{\partial y} = 0 \tag{2.1}$$

and

$$\frac{\partial u}{\partial t} + u\,\frac{\partial u}{\partial x} + v\,\frac{\partial u}{\partial y} = -\,\frac{1}{\rho}\,\frac{\partial P}{\partial x} + gx\beta(T - T_0) + \nu\,\frac{\partial^2 u}{\partial y^2}\,. \tag{2.2}$$

These two equations, known as the continuity and momentum, or Navier Stokes equations, must be augmented by the energy equation when information concerning the temperature distributions in the boundary layer is required. The energy equation, in general form [12], can be written as

$$\rho C_P\,\frac{\partial T}{\partial t} + \rho C_P\left(u\,\frac{\partial T}{\partial x} + v\,\frac{\partial T}{\partial y}\right) = K\,\frac{\partial^2 T}{\partial y^2} + \beta TU\,\frac{dP}{dx} + \mu\left(\frac{\partial u}{\partial y}\right)^2 - \nabla\cdot\vec{q}_r\,. \tag{2.3}$$

In this expression, the quantity $\vec{q}_r$ refers to heat flux due to thermal radiation, and the pressure term on the right is associated with buoyant forces evident in situations involving free convection.

It would be advantageous at this point to digress momentarily in an effort to establish the fundamental considerations and assumptions which must be used in applying these equations to solution of the flow field in the free jet boundary. First of all, since the flow field to be investigated possesses a curved geometry, some ease of manipulation may be gained through use of curvilinear coordinates. Additionally, the case where thermal radiation and high temperatures are present provides another simplification in that buoyant forces normally associated with free convection are negligible. These high temperatures also allow some reasonable assumptions concerning the neglect of dissipation effects, primarily due to the fact that these effects are small when compared to other transfer mechanisms in the flow. Finally, the analysis may be further simplified through the assumption that the flow velocity is constant with respect to time. This last statement could not, of course, be considered as absolute, since in the case of a fully turbulent flow, small fluctuations in the flow velocity will always exist at any given instant in time. Further discussion of how these fluctuations may be treated will be provided later in section C of this chapter.

In the case of radiating media, the degree to which the medium in question is capable of absorbing radiation has a definite effect on the extent of radiation transfer within the medium. This capability for radiation transport is known as the optical thickness of the medium. In an optically thick medium, for example, radiation emitted from individual molecules affects only molecules in close proximity. The parameter of optical thickness, according to Sparrow and Cess [12], is defined as the ratio of the photon mean free path to some characteristic length in the radiating medium. Findings [9] indicate that if consideration is confined to an optically thick medium, the so-called Rosseland approximation to the radiation heat flux q_r may be employed. This approximation is given by the expression

$$q_r = - \frac{4\lambda^2\sigma}{3\kappa} \frac{\partial T^4}{\partial y}$$

where κ is the absorptivity of the medium, σ is the Stefan Boltzman constant and λ is the wavelength of the emitted radiation.

A re-examination of Equations (2.1) - (2.3) with application of the above considerations and assumptions allows a number of simplifications to be made. In Equation (2.2) the time derivative may be ignored as a result of steady flow, and the buoyancy term $gx\beta(T - T_0)$, may be ignored as a negligible effect to yield the result

$$u \frac{\partial u}{\partial x} + v \frac{\partial u}{\partial y} = - \frac{1}{\rho} \frac{\partial P}{\partial x} + \nu \frac{\partial^2 u}{\partial y^2} . \tag{2.4}$$

Likewise, the time derivative and buoyancy terms may be deleted in Equation (2.3) along with the dissipation term, $\mu \left(\frac{\partial u}{\partial y} \right)^2$. The optically thick assumption also permits substitution for the radiative heat flux, $\vec{q}_r$, so that the energy equation becomes

$$\rho C_P \left(u \frac{\partial T}{\partial x} + v \frac{\partial T}{\partial y} \right) = K \frac{\partial^2 T}{\partial y^2} - \frac{\partial}{\partial y} \left(- \frac{4\lambda^2 \sigma}{3\kappa} \frac{\partial T^4}{\partial y} \right) ,$$

where the product $\nabla \cdot \vec{q}_r$ has been expressed in terms of its y scalar component. Then the energy equation takes as its final form

$$\rho C_P \left(u \frac{\partial T}{\partial x} + v \frac{\partial T}{\partial y} \right) = K \frac{\partial^2 T}{\partial y^2} + \frac{4\lambda^2 \sigma}{3\kappa} \frac{\partial^2 T^4}{\partial y^2} . \tag{2.5}$$

One additional relationship connecting curvature and pressure gradients normal to a curved surface in a flow has been introduced and used in the analysis of curved flow fields by a number of reserachers [2, 5, 6]. This expression,

$$Ru^2 = \frac{1}{\rho} \frac{\partial P}{\partial y} , \tag{2.6}$$

relates the pressure gradient normal to the direction of flow to the flow velocity, u, and the curvature, R, in cases where the curvature is moderate. This equation, along with Equations (2.1), (2.4), and (2.5), form the complete set of equations required to specify the solution to the problems of momentum and heat transfer in the free jet boundary. Briefly restated they are:

$$\frac{\partial u}{\partial x} + \frac{\partial v}{\partial y} = 0 \tag{2.1}$$

$$u \frac{\partial u}{\partial x} + v \frac{\partial u}{\partial y} = - \frac{1}{\rho} \frac{\partial P}{\partial x} + \nu \frac{\partial^2 u}{\partial y^2} \tag{2.4}$$

$$\rho C_P \left(u \frac{\partial T}{\partial x} + v \frac{\partial T}{\partial y} \right) = K \frac{\partial^2 T}{\partial y^2} + \frac{4\lambda^2 \sigma}{3\kappa} \frac{\partial^2 T^4}{\partial y^2} \tag{2.5}$$

$$Ru^2 = \frac{1}{\rho} \frac{\partial P}{\partial y} . \tag{2.6}$$

A physical interpretation of the flow field and the boundary conditions which apply can be visualized by reference to Figure 1. As shown, the moving fluid which has already established a fully developed flow profile possesses a freestream velocity U_{max} and a bulk fluid temperature T_∞ before it reaches the region of stagnant fluid which has velocity $u = 0$ and a bulk fluid temperature T_S. A short distance beyond the point of issue which may be denoted as x_0, entrainment of the stagnant fluid causes alteration of velocity and temperature profiles such that at large

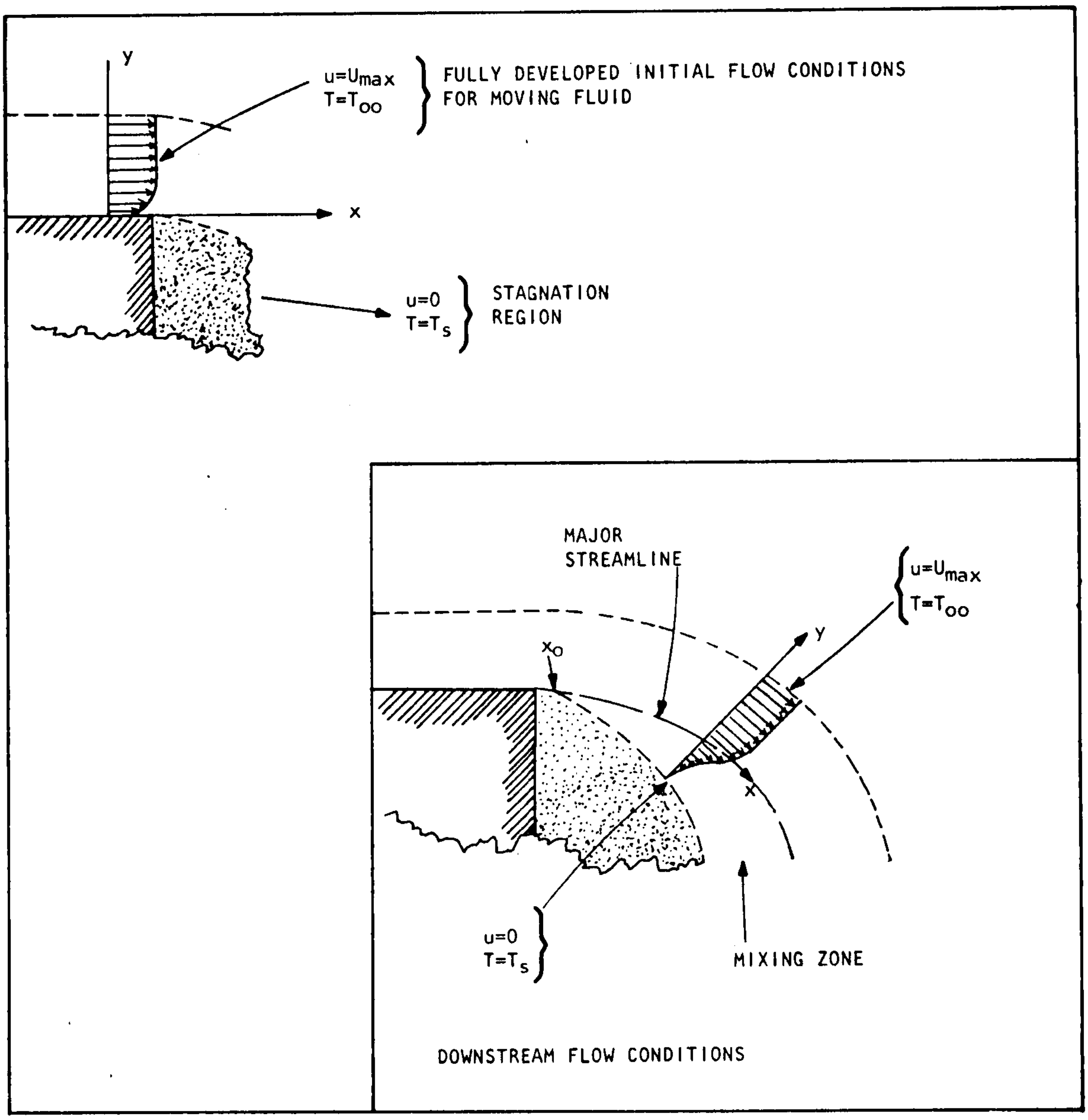

Figure 1. Flow Profile for Initial and Downstream Conditions.

negative values of $y(y \rightarrow -\infty)$, $u = 0$ and $T = T_s$. Alternately, at large positive values of $y(y \rightarrow +\infty)$, freestream conditions again prevail. The condition of constant curvature along the major streamline which also serves as the abscissa in the curvilinear coordinate system provides that the velocity normal to the direction of flow (v) is also zero at this point.

Reference 5 provides velocity profiles for a curved free jet boundary flow field through solution of Equations (2.1), (2.4), and (2.6) by using a similarity transformation technique for conditions of laminar and turbulent flow. As this information is vital in the establishment of temperature profiles for this type of flow field, frequent use will be made of the transformed differential equation given for the similar velocity profiles. Only brief treatment will be given here to development of the transformed momentum equation. This is done primarily to provide clarity and consistency to the present discussion while it avoids lengthy repetitions of what can already be found in the literature.

B. Laminar Flow Fields

In the case of laminar flow, the boundary layer equations outlined above can provide a representation of the velocity distributions to be found in the curved free jet boundary through the treatment to be outlined in the following discussion. First of all, differentiation of Equation (2.4) with respect to y gives

$$\frac{\partial u}{\partial x}\frac{\partial u}{\partial y} + u\frac{\partial^2 u}{\partial x \partial y} + \frac{\partial v}{\partial y}\frac{\partial u}{\partial y} + v\frac{\partial^2 u}{\partial y^2} = -\frac{1}{\rho}\frac{\partial^2 P}{\partial x \partial y} + \nu\frac{\partial}{\partial y}\left(\frac{\partial^2 u}{\partial y^2}\right) .$$

Likewise differentiation of Equation (2.6) with respect to x gives

$$u^2\frac{\partial R}{\partial x} + 2Ru\frac{\partial u}{\partial x} = \frac{1}{\rho}\frac{\partial^2 P}{\partial x \partial y} .$$

Note that the common term $\frac{1}{\rho}\frac{\partial^2 P}{\partial x \partial y}$ in both equations allows an equivalence to be established for the two. Further, Equation (2.1) shows that

$$\frac{\partial u}{\partial x} = -\frac{\partial v}{\partial y} .$$

These three relationships can now be combined to provide the following single partial differential equation:

$$\frac{\partial u}{\partial x}\frac{\partial u}{\partial y} + u\frac{\partial^2 u}{\partial x \partial y} - \frac{\partial u}{\partial x}\frac{\partial u}{\partial y} + v\frac{\partial^2 u}{\partial y^2} = -2Ru\frac{\partial u}{\partial x} - u^2\frac{\partial R}{\partial x} + \nu\frac{\partial^3 u}{\partial y^3} .$$

The simplified form of this equation then becomes

$$u\frac{\partial^2 u}{\partial x \partial y} + v\frac{\partial^2 u}{\partial y^2} = -2Ru\frac{\partial u}{\partial x} - u^2\frac{dR}{dx} + \nu\frac{\partial^3 u}{\partial y^3} . \qquad (2.7)$$

The term $- u^2 \frac{\partial R}{\partial x}$ has been written as a total derivative here since in the curvilinear coordinate system under consideration the curvature has been restricted to be a function of displacement, x, along the major streamline.

The process of transforming this partial differential equation into a more tractable ordinary differential equation can be initiated through definition of the stream function, ψ, where

$$\psi = (U_1 \nu x)^{1/2} f(\eta) \quad , \tag{2.8a}$$

and

$$\eta = y(U_1/\nu x)^{1/2} \quad . \tag{2.8b}$$

The quantity U_1 is the velocity along the major streamline. A transformation parameter for the curvature can be defined in a similar manner such that

$$R = (R_0/x)^{1/2} \quad . \tag{2.9}$$

Expressions for the flow velocities u and v may now be obtained as follows:

$$u = \frac{\partial \psi}{\partial y} = \frac{\partial}{\partial y}\left[(U_1 \nu x)^{1/2} f(\eta)\right] = U_1 f' \tag{2.10a}$$

$$v = - \frac{\partial \psi}{\partial x} = - \frac{\partial}{\partial x}\left[(U_1 \nu x)^{1/2} f(\eta)\right] = \frac{1}{2}\left\{(U_1 \nu/x)^{1/2} (\eta f' - f)\right\} \quad . \tag{2.10b}$$

Substitution of the expressions in Equations (2.10) into Equation (2.7) will, after much effort, give an ordinary differential equation of the form

$$2f^{iv} + f'f'' + ff''' + (R_0\nu/U_1)^{1/2}[f'^2 + 2\eta f'f''] = 0 \ . \tag{2.11}$$

Solution of this equation will then provide the velocity profile for laminar flow in the curved free jet boundary.

Attention can now be turned to reduction of the energy equation (Eq. 2.5) to ordinary differential form by first assuming that, for purposes of transformation, the stream function defining the velocities u and v is still valid and that $T(x,y) = T(\eta)$. The thermal diffusivity, α, is expressed by the relation $\alpha = \frac{K}{\rho C_p}$ so that Equation (2.5) can be rewritten as

$$u\frac{\partial T}{\partial x} + v\frac{\partial T}{\partial y} = \frac{\partial^2 T}{\partial y^2} + \frac{4\lambda^2\sigma}{3\kappa\rho C_p}\frac{\partial^2 T^4}{\partial y^2} \ .$$

The effects of nonlinearity which appear due to the term T^4 can be dealt with by making use of a linearizing technique. If it is assumed that the temperature range over the flow field is small, then T^4 may be expressed as a linear function of temperature by expanding T^4 about T_∞ in a Taylor series. Neglecting higher order terms in the expansion results in the approximating expression

$$T^4 \approx 4T_\infty^3 \; T - 3T_\infty^4 \; .$$

With this in mind, the energy equation can be expressed by

$$u \frac{\partial T}{\partial x} + v \frac{\partial T}{\partial y} = \alpha \frac{\partial^2 T}{\partial y^2} + \frac{4\lambda^2 \sigma}{3\kappa \rho C_P} \frac{\partial^2}{\partial y^2} (4T_\infty^3 \; T - 3T_\infty^4) \; ,$$

which reduces to

$$u \frac{\partial T}{\partial x} + v \frac{\partial T}{\partial y} = \alpha \frac{\partial^2 T}{\partial y^2} + \frac{4\lambda^2 \sigma}{3\kappa \rho C_P} \cdot 4T_\infty^3 \frac{\partial^2 T}{\partial y^2} \; .$$

The above equation can now be recast in terms of similarity variables by recalling u and v from Equations (2.10) and by performing the following transformations for T:

$$\frac{\partial T}{\partial x} = \frac{\partial T}{\partial \eta} \frac{\partial \eta}{\partial x} = T' \frac{\partial}{\partial x} \, y(U_1/\nu x)^{1/2}$$

$$= T' \; [1/2(U_1/\nu x)^{-1/2}(-U_1/\nu x^2)]y$$

$$= - \; 1/2 \; x \; (T'\eta)$$

and

$$\frac{\partial T}{\partial y} = \frac{\partial T}{\partial \eta} \frac{\partial \eta}{\partial y} = T' \; (U_1/\nu x)^{1/2} \; .$$

The left side of the energy equation in terms of transformed variables, then, is

$$- \frac{U_1}{2x} f'\eta T' + \frac{1}{2} \left(\frac{U_1 \nu}{x}\right)^{1/2} [\eta f' - f] \; T' \left(\frac{U_1}{\nu x}\right)^{1/2} \; .$$

The right side of the equation can now be expanded through the following:

$$\alpha \frac{\partial^2 T}{\partial y^2} + \frac{4\lambda^2\sigma}{3\kappa\rho C_p} \cdot 4T_\infty^3 \frac{\partial^2 T}{\partial y^2} = \left(\alpha + \frac{4\lambda^2\sigma}{3\kappa\rho C_p} \cdot 4T_\infty^3\right) \frac{\partial^2 T}{\partial y^2} .$$

Performing the variable transformation gives

$$\left(\alpha + \frac{4\lambda^2\sigma}{3\kappa\rho C_p} \cdot 4T_\infty^3\right) \frac{\partial}{\partial y} T' \left(\frac{U_1}{\nu x}\right)^{1/2}$$

or

$$\left(\alpha + \frac{4\lambda^2\sigma}{3\kappa\rho C_p} \cdot 4T_\infty^3\right) T'' \left(\frac{U_1}{\nu x}\right) .$$

The complete energy equation in terms of similarity variables then becomes

$$-\frac{U_1}{2x} f'\eta T' + \frac{U_1}{2x} [\eta f' - f]T' = \frac{U_1}{\nu x} \left(\alpha + \frac{4\lambda^2\sigma}{3\kappa\rho C_p} \cdot 4T_\infty^3\right) T'' .$$

Further cancellation of terms and reduction of the left side of the equation results in the more simplified expression

$$-\frac{U_1}{2x} fT' = \frac{U_1}{\nu x} T'' \left(\alpha + \frac{4\lambda^2\sigma}{3\kappa\rho C_p} \cdot 4T_\infty^3\right) ,$$

which ultimately leads to

$$-fT' = 2T'' \left(\frac{\alpha}{\nu} + \frac{4\lambda^2\sigma}{3\kappa\nu\rho C_p} \cdot 4T_\infty^3\right) . \tag{2.12}$$

Further examination of Equation (2.12) reveals some interesting possibilities. First of all, the dimensionless quantity known as the Prandtl number, Pr, is defined by the expression $Pr = \frac{\mu C_p}{K}$. Then $\frac{\alpha}{\nu} = \frac{K\rho}{\mu\rho C_p} = \frac{1}{Pr}$. In the second term on the right side, the quantity $\nu\rho C_p$ appears and can be written as $\frac{\mu}{\rho}\rho C_p = \mu C_p$. Then it is apparent that the constants on the right side may be written as

$$\frac{\alpha}{\nu} = \frac{1}{Pr} , \tag{2.13a}$$

$$\frac{16\lambda^2\sigma T_\infty^3}{3\kappa\mu C_p} = \frac{16\lambda^2\sigma T_\infty^3}{3\kappa K Pr} . \tag{2.13b}$$

Use of these expressions in Equation (2.12) yields

$$- fT' = \frac{2T''}{Pr}\left(1 + \frac{16\lambda^2\sigma T_\infty^3}{3\kappa K}\right) .$$

Sparrow and Cess [12] define a dimensionless quantity, N, called the conduction-to-radiation parameter which depicts the relative contributions of conduction and radiation to the heat transfer process. This quantity is defined as

$$N = \frac{\kappa K}{4\lambda^2\sigma T_\infty^3} .$$

Incorporation into the transformed energy equation reduces it to

$$\frac{2}{Pr}\left(1 + \frac{4}{3N}\right) T'' + fT' = 0$$

or

$$\left(1 + \frac{4}{3N}\right) T'' + \frac{Prf}{2} T' = 0 \ . \tag{2.14}$$

Hence, an ordinary differential equation has been formed which will provide a temperature distribution in the flow field in terms of the similarity variable η.

It is also desirable to express the temperature $T(\eta)$ in terms of a nondimensional entity; thus one may define the temperature, θ, such that $\theta = \frac{T(\eta) - T_s}{T_\infty - T_s}$. Then, for $T(\eta) = \theta(T_\infty - T_s) + T_s$, it is seen that

$$T' = \frac{dT}{d\eta} = \theta'(T_\infty - T_s) \tag{2.15a}$$

and

$$T'' = \frac{d^2T}{d\eta^2} = \theta''(T_\infty - T_s) \ . \tag{2.15b}$$

Finally, with substitutions to nondimensionalize Equation (2.14), one finds that

$$\left(1 + \frac{4}{3N}\right) \theta''(T_\infty - T_s) + \frac{Prf}{2} \theta' (T_\infty - T_s) = 0 \ ,$$

which upon further simplification leaves

$$\left(1 + \frac{4}{3N}\right)\theta'' + \frac{Prf}{2} \theta' = 0 \ . \tag{2.16}$$

A short review of the boundary conditions for this equation is in order. Recall that at large negative values of y ($y \rightarrow -\infty$) the temperature will approach that of the stagnant medium into which the jet issues; hence at $y = -\infty$, $T(x,-\infty) = T_s$. In dimensionless transformation this boundary condition becomes

$$\lim_{\eta \to -\infty} \theta = \frac{T_s - T_s}{T_\infty - T_s} = 0 \ .$$

On the other hand, at large positive y ($y \rightarrow +\infty$) the temperature in the flow is assumed to be that of the bulk fluid such that at $y = +\infty$, $T(x, +\infty) = T_\infty$, or in dimensionless form

$$\lim_{\eta \to +\infty} \theta = \frac{T_\infty - T_s}{T_\infty - T_s} = 1 \ .$$

Now that the form of the ordinary differential equation has been specified along with its boundary conditions, one need only determine the form of the dimensionless stream function, f, from the momentum equation to determine the temperature profile in the laminar flow field.

C. Turbulent Flow Fields

For turbulent flow, one must define additional coefficients which describe the effects of turbulent transport processes on the momentum and thermal energy in the system. These effects are seen in the thermal conductivity K and the dynamic viscosity μ. In a medium where turbulent flow prevails, there exists a very thin laminar viscous layer close to the interface of the boundary and the containing surface such that the shear flow in this region can be described through a superposition of the effects of the laminar viscosity, μ, and the turbulent eddy viscosity, ε. The total effect for shear stress then can be seen as

$$\tau = (\mu + \varepsilon) \frac{\partial u}{\partial y} .$$

Thus, for turbulent flows, the last term in Equation (2.4) has the form

$$\frac{1}{\rho} (\mu + \varepsilon) \frac{\partial^2 u}{\partial y^2} .$$

In the case of the free jet boundary, the absence of a wall at the boundary renders the effects of the laminar interface negligible so that contributions from μ can be omitted. Also, the time average of the fluctuations in the system reduce to an expression where only the mean motion of the flow is important. If the mean velocity in the x direction is denoted as $\bar{u}$ and in the y direction as $\bar{v}$ then Equation (2.4) can be written as

$$\bar{u} \frac{\partial \bar{u}}{\partial x} + \bar{v} \frac{\partial \bar{u}}{\partial y} = - \frac{1}{\rho} \frac{\partial \bar{P}}{\partial x} + \frac{1}{\rho} \varepsilon \frac{\partial^2 \bar{u}}{\partial y^2} . \tag{2.17}$$

It is known that, unlike the viscosity, μ, which is a property of the fluid, the eddy viscosity, ε, depends heavily on the turbulent activity in the flow. Introduction of an argument from Prandtl's mixing length theories will allow evaluation of ε for the free turbulent flow considered here. Prandtl postulated that the turbulent eddy viscosity is proportional to the maximum difference in the mean flow velocities and the mixing length, l, of the region of turbulence, or

$$\varepsilon = cl(U_{max} - U_{min}) \ ,$$

where c is a constant of proportionality. In the present case, of course, flow into a stagnant region indicates that $U_{min} = 0$ so that the representation for ε becomes

$$\varepsilon = clU_{max} \ .$$

Since the mixing length, l, is also proportional to the displacement, x, along the curvilinear axis of the flow, then l may be replaced by a suitable constant times the downstream displacement to yield

$$\varepsilon = czxU_{max} \ .$$

Substitution into Equation (2.17) above now provides an expression which accounts for turbulent effects in the momentum transfer process in the free jet boundary. The turbulent form of Equation (2.6) can now be cross differentiated along with Equation (2.17) and the two combined through a substitution from the continuity equation (Eq. 2.1) in a manner similar to that discussed in the previous section so that a single partial differential equation is obtained. This equation has the form of Equation (2.7) with the exception that the last term will be

$$\frac{1}{\rho}(czxU_{max}) \frac{\partial^3 \overline{u}}{\partial y^3} .$$

Williams, Cheng and Kim [5] showed that, provided the curvature, R, is assumed to vary inversely with displacement x, a similarity transformation could be obtained through use of the following transformation parameters:

$$\psi = \frac{1}{(2)^{1/2}} \left(\frac{x}{\omega}\right) U_1 f(\eta) \ , \ \eta = (2)^{1/2} \left(\frac{\omega}{x}\right) y \tag{2.18a}$$

$$R = \frac{R_0}{x} . \tag{2.18b}$$

The free constant, ω, if specified according to [5] as

$$\omega = \left(729 \frac{U_1}{U_{max}}\right)^{1/2}$$

reduces the transformed differential equation to

$$2f'^{v} + f'f'' + ff''' + \left[\frac{R_0}{2^{1/2}}\right] \omega \, (f'^2 + 2\eta f'f'') = 0 \; . \tag{2.19}$$

Comparison of Equation (2.19) with Equation (2.11) reveals that they are identical with the exception of the form of the constant in the last term.

Again, if it is assumed that the transformation parameters above are valid for the energy equation and that $T(x, y) = T(\eta)$, the search for an expression relating heat transfer in a turbulent flow field can proceed. Just as turbulence affects viscosity, however, one must consider the effects of turbulence on thermal properties before the problem at hand may be attacked properly. In most turbulent flows, a thin portion of the boundary layer exists where thermal conductivity is the result of the superposition of a laminar conductivity K and a turbulent conductivity which shall be defined as π. Hence the heat flux across the boundary due to conductivity can be given by

$$q_c = (K + \pi) \frac{\partial \overline{T}}{\partial y} \; .$$

Recalling the convention for turbulent mean flows and negligible laminar effects in free turbulent flows then, Equation (2.5) can be expressed as

$$\rho C_p \left(\overline{u} \frac{\partial \overline{T}}{\partial x} + \overline{v} \frac{\partial \overline{T}}{\partial y}\right) = \pi \frac{\partial^2 \overline{T}}{\partial y^2} + \frac{4\lambda^2 \sigma}{3\kappa} \frac{\partial^2 \overline{T}^4}{\partial y^2} \; . \tag{2.20}$$

Now, using the transformation variables,

$$\bar{u} = \frac{\partial\psi}{\partial y} = U_1 f' \ , \tag{2.21a}$$

$$\bar{v} = -\frac{\partial\psi}{\partial x} = \left[\frac{U_1}{2^{1/2}\omega}\right] (f'\eta - f) \ , \tag{2.21b}$$

and

$$\bar{T}(x,y) = \bar{T}(\eta) \ . \tag{2.21c}$$

Derivatives of $\bar{T}$ in terms of transformed variables are

$$\frac{\partial\bar{T}(\eta)}{\partial x} = \bar{T}' \frac{\partial}{\partial x}\left[\frac{2^{1/2}\omega y}{x}\right]$$

$$= -\bar{T}' 2^{1/2} \frac{\omega y}{x^2} \text{ or } -\frac{\eta\bar{T}'}{x} \ , \tag{2.22a}$$

and

$$\frac{\partial\bar{T}}{\partial y} = \bar{T}' \frac{\partial}{\partial y}\left[\frac{2^{1/2}\omega y}{x}\right]$$

$$= \bar{T}' \frac{2^{1/2}\omega}{x} \ . \tag{2.22b}$$

Application of these expressions to the left side of Equation (2.20) first gives

$$\rho C_p \left[U_1 f'\left(\eta \frac{\bar{T}'}{x}\right) + \left(\frac{U_1}{2^{1/2}\omega}\right)(f'\eta - f)\left(\frac{\bar{T}' 2^{1/2}\omega}{x}\right)\right]$$

such that

$$\rho C_p \left[-\frac{U_1 \eta f'\bar{T}'}{x} + \frac{U_1 \eta f'\bar{T}'}{x} - \frac{U_1 f\bar{T}'}{x}\right] = -\rho C_p \frac{U_1 f\bar{T}'}{x} \ .$$

The second derivatives on the right hand side of Equation (2.20) are evaluated as

$$\frac{\partial}{\partial y}\left(\bar{T}' \, \frac{2^{1/2}\omega}{x}\right) = \frac{2^{1/2}\omega}{x}\,\bar{T}''\left(\frac{2^{1/2}\omega}{x}\right)$$

$$= \left(\frac{2\omega^2}{x^2}\right)\bar{T}'' \; ,$$

and as

$$\frac{\partial^2 \bar{T}^4}{\partial y^2} = \frac{\partial^2}{\partial y^2}\,(4\bar{T}_\infty^3\bar{T} - 3\bar{T}_\infty^4)$$

$$= 4\bar{T}_\infty^3\,\frac{\partial \bar{T}'}{\partial y}\left(\frac{2^{1/2}\omega}{x}\right)$$

$$= 4\bar{T}_\infty^3\bar{T}''\left(\frac{2\omega^2}{x^2}\right) .$$

Thus the completely expanded energy equation is

$$-\rho C_p\,\frac{U_1 f\bar{T}'}{x} = \frac{2\omega^2}{x^2}\left[\pi\;\bar{T}'' + \frac{4\lambda^2\sigma}{3\kappa}\cdot 4\;\bar{T}_\infty^3\;\bar{T}''\right] . \qquad (2.23)$$

Arguments from Prandtl and others [1] may once again be used to simplify things at this point. Prandtl argued that the same mechanism which controlled momentum transfer in turbulent flows also controlled the transfer of heat. Thus, the turbulent conductivity, π, defined by the relationship $\pi = C_p\,A_q$ can also be related to the mixing length l through the eddy viscosity, ε. Here, A_q is a constant dependent upon the level of turbulence in the flow. The eddy viscosity can be considered similar to the kinematic viscosity ν. The analogy to the laminar case then can be seen through the expression

$$\varepsilon = \frac{A_\tau}{\rho}$$

where A_τ corresponds to μ. Division of Equation (2.23) by ρC_p and substitution for π gives

$$-\frac{U_1 f\bar{T}'}{x} = \frac{2\omega^2}{x^2}\left[\frac{C_p A_q}{\rho C_p}\bar{T}'' + \frac{16\lambda^2\sigma}{3\kappa\rho C_p}\bar{T}''\right] . \qquad (2.24)$$

Examination of the first term on the right reveals that introduction of another dimensionless parameter called the turbulent Prandtl number, and defined by the expression

$$P_t = \frac{A_\tau}{A_q} ,$$

will assist in simplifying the differential equation. Recall also from the discussion on eddy viscosity that

$$\frac{1}{\rho} = \frac{\varepsilon}{A_\tau} .$$

The constant for the first term on the right can then be written as

$$\frac{A_q}{\rho} = A_q \cdot \frac{\varepsilon}{A_\tau}$$

$$= \frac{\varepsilon}{P_t} \, .$$

Turning attention to the second term on the right and using the relationships developed above, it is easily seen that

$$\frac{16\lambda^2\sigma}{3\kappa\rho C_p} = \frac{16\lambda^2\sigma}{\frac{3\kappa A_\tau C_p}{\varepsilon}} \, , \text{ or}$$

$$\frac{16\lambda^2\sigma\varepsilon}{3\kappa A_\tau C_p} \cdot \frac{A_q}{A_q} = \frac{\varepsilon}{P_t} \cdot \frac{16\lambda^2\sigma}{3\kappa\pi} \, .$$

Incorporation of these simplifications into Equation (2.24) yields

$$- \frac{U_1 f\overline{T}'}{x} = \frac{2\omega^2}{x^2} \frac{\varepsilon}{P_t} \left[\overline{T}'' + \frac{16\lambda^2\sigma}{3\kappa\pi} \overline{T}_\infty^3 \, \overline{T}'' \right] \, .$$

The value for ε has already been shown to be $czxU_{max}$, and the constant ω to be $(729 \; U_1/U_{max})^{1/2}$ for reduction of the momentum equation. If it is assumed, as Prandtl suggests, that mechanisms in turbulent momentum and heat transfer are the same, then these constants will have the same values in the energy equation. Therefore,

$$- \frac{U_1 f\overline{T}'}{x} = \frac{2}{x^2} \left(729 \frac{U_1}{U_{max}} \right) \left(\frac{xU_{max}}{729P_t} \right) \left[\overline{T}'' + \frac{16\lambda^2\sigma}{3\kappa\pi} \overline{T}_\infty^3 \, \overline{T}'' \right] \, ,$$

which reduces to

$$- f\overline{T}' = \frac{2}{P_t}\left[\overline{T}'' + \frac{16\lambda^2\sigma}{3\kappa\pi}\,\overline{T}_\infty^3\,\overline{T}''\right] .$$

Finally, examination of the term, $\frac{16\lambda^2\sigma}{3\kappa\pi}$, indicates that just as in the laminar case, a turbulent conduction-to-radiation parameter N may be defined based on the conductivity parameter, π, as follows:

$$N = \frac{\kappa\pi}{4\lambda^2\sigma\overline{T}_\infty^3} .$$

Substitution for this parameter in the energy equation results in the final form

$$\frac{2}{P_t}\left(1 + \frac{4}{3N}\right)\overline{T}'' = - f\overline{T}' . \qquad (2.25)$$

This equation can be nondimensionalized in the same manner as Equation (2.14) by specifying that $\theta = \frac{T(\eta) - Ts}{T_\infty - Ts}$. The resulting expression is seen to be

$$\frac{2}{P_t}\left(1 + \frac{4}{3N}\right)\theta''(\overline{T}_\infty - \overline{T}_s) = f\theta'(\overline{T}_\infty - \overline{T}_s) ,$$

where a slight rearrangement of terms gives

$$\left(1 + \frac{4}{3N}\right)\theta'' + \frac{P_t f}{2}\theta' = 0 . \qquad (2.26)$$

The above equation is identical to that derived for conditions of laminar flow in the free jet boundary with the exception that the mean temperature distribution $\overline{T}$ is included and that the turbulent conduction-to-radiation parameter N makes use of the turbulent conductivity π rather than the conventional coefficient K. The boundary conditions for this situation, however, remain identical to those for the laminar case. Therefore, solution of either Equation (2.16) or Equation (2.26) will provide representative temperature profiles for the curved free jet boundary.

CHAPTER III

ANALYSIS OF THE SIMILARITY SOLUTION

A. Solution of the Momentum Equation

It was noted in Chapter II that Equations (2.11) and (2.19) are identical with the exception of the constant which contains the local curvature, R_0. In either case, this constant provides the relative influence of local curvature on the similarity velocity profile without regard as to whether the flow is laminar or turbulent in nature. Thus, if a curvature parameter, $\mathcal{R}$, is defined such that for laminar flow

$$\mathcal{R} = \left(\frac{R_0 \nu}{U_1}\right)^{1/2} ,$$

and for turbulent flow

$$\mathcal{R} = \left(\frac{R_0}{2^{1/2}}\right)\omega ,$$

the singular expression for the fourth order ordinary differential equation to be solved becomes

$$2f^{iv} + f'f'' + ff''' + \mathcal{R}(f'^2 + 2\eta f'f'') = 0 .$$

This equation can be rewritten as

$$2\frac{d}{d\eta}f''' + \frac{d}{d\eta}(ff'') + \mathcal{R}\frac{d}{d\eta}(\eta f'^2) = 0 ,$$

which when integrated once yields

$$2f''' + ff'' + R\eta f'^2 = C_1 \ . \qquad (3.1)$$

Examination of the boundary conditions at $\eta = -\infty$ indicates that the value of the integration constant, C_1, should be zero since at this point both f' and f'' are zero. The resulting restriction on f''' at this point is obvious:

$$f''' (-\infty) = 0 \Rightarrow C_1 = 0 \ .$$

The final form of the equation to be dealt with for the velocity profile solution is

$$2f''' + ff'' + R\eta f'^2 = 0 \ . \qquad (3.2)$$

This equation is nonlinear and does not readily yield to analytical solution. Furthermore, not enough boundary conditions are specified to determine all the constants of integration even if one were fortunate enough to arrive at an analytical form for $f(\eta)$.

In spite of the difficulties involved in the solution of this type of equation, extremely good results have been obtained through use of numerical techniques. Consider, for example, the case where $R = 0$ in Equation (3.2) above. The resulting form of the equation can be recognized as the celebrated Blasius equation for flow over a flat plate.

Numerous references to numerical solution of this equation may be found in the literature addressing viscous flows. The difference between the Blasius solution and the one sought in this study, however, can be found in specification of the boundary conditions. The present problem must be attacked in two parts, one which utilizes the constraints placed on the function in the interval, $(0, -\infty)$, and the other which examines the behavior of the function in the interval, $(0, +\infty)$.

Employment of any numerical scheme to arrive at a solution to the equation will require complete specification of boundary conditions at both the starting and ending points of the interval. In the current situation, the third order equation requires constraints for f, f' and f''. At $\eta = -\infty$, the requirement that $f' = 0$ due to its asymptotic approach automatically requires that $f'' = 0$, and provides justification to state that, at most, f must approach some constant value. On the other hand, at $\eta = 0$, f and f' are specified as 0 and 1 respectively but no requirements are given for f''. It is mundane to the solution of the problem, however, that $f''(0)$ must be given a specific value if the conditions at $-\infty$ are to be met. Thus, one would have to approach this part of the problem solution with an "educated guess" at the value of $f''(0)$ and see if the conditions at $\eta = -\infty$ can be met.

Correct determination of the value of $f''(0)$ for the interval, $(0, -\infty)$, provides a bit more ease in finding the solution on $(0, +\infty)$ since all needed parameters at the starting point of the second solution interval will have already been furnished. The major consideration on this interval is the point at which the influence of the curvature parameter becomes dominant in the solution. This point is specified by the outer boundary condition for the mixing zone as

$$\frac{f''}{f'} = -R \ .$$

Beyond this point, the matching of the boundary layer profile with the freestream velocity is governed primarily by curvature. Hence, analytical solution of the outer boundary condition with constants of integration specified at the point where the condition first becomes valid will yield a solution curve for the remainder of the solution interval.

The analytical solution to the boundary condition may be outlined as follows. First of all, rearrangement of the expression gives

$$f'' + Rf' = 0 \ .$$

This differential equation can be recognized as having general solutions of two differing forms depending on the value of R. For instance, if $R = 0$ (designated Case I), the equation becomes

$$f'' = 0 ,$$

and the general solution takes the form

$$f = \beta_1 \eta + \beta_2 . \tag{3.3}$$

The curve of interest, $f'(\eta)$, which is that of the velocity profile, can be generated simply by taking the derivative with respect to η to get

$$f' = \beta_1 . \tag{3.4}$$

This last expression shows that for $R = 0$, the value of $f'(\eta)$ is constant for all η once the outer boundary condition is satisfied, and that the integration constants, β_1 and β_2, can be determined by knowing the value of $f'(\eta)$ for which the slope (f'') of the velocity profile is zero.

Case II for this equation occurs when $|R|>0$. The general solution, then, can be found by using the method of undetermined coefficients. First condider that the expression for the boundary condition can be rewritten as

$$\frac{d}{d\eta}(\ln f') = - R .$$

Integration gives

$$\ln f' = - R\eta + \gamma ,$$

where γ is a constant of integration. Simplification gives

$$f' = e^{\gamma} e^{-R\eta}$$

or

$$f' = \beta_1 e^{-R\eta} \quad . \tag{3.5}$$

Further, the general solution to the linear Equation (3.5) above can be expressed as the sum of the solution, f_h, to the homogeneous equation, $f' = 0$, and the complementary solution f_p. The method of undetermined coefficients allows the assumption that, for the differential equation of form

$$L(f) = \phi(\eta) = e^{\alpha\eta} P_n(\eta) \quad ,$$

the complementary solution f_p has the form

$$f_p = e^{\alpha\eta} (A_n \eta^n + A_{n-1} \eta^{n-1} + . . . + A_1 \eta + A_0) \; .$$

In the equations above, $P_n(\eta)$ is an nth degree polynomial with coefficients A_0, ... A_n as shown. The form of $\phi(\eta)$ in the case under consideration is

$$\phi(\eta) = \beta_1 e^{-R\eta}$$

such that the explicit form of f_p becomes

$$f_p = \beta_1 e^{-R\eta} \; .$$

This form of f_p is compatible with the general form if one considers the constant β_1 to be a polynomial of degree zero. The homogeneous solution can be written as

$$f_h(\eta) = \beta_2 \; .$$

Thus, the complete solution for Case II is $f = \beta_1 \, e^{-R\eta} + \beta_2$, and, as before, the constants, β_1 and β_2, are determined at the point where the outer boundary condition becomes valid.

B. Solution of the Energy Equation

Equations (2.16) and (2.26) provide similar forms of the differential equation to be solved for the temperature distribution over the solution interval in question. The differences in these two equations, as explained at the conclusion of Chapter II, are seen only in the manner in which they describe the mechanical processes taking place in the flow field. Their mathematical solution is identical in that for cases where $Pr = P_t$ and the values of N for the laminar equation (Eq. 2.16) and the turbulent equation (Eq. 2.26) are the same, solution of either will produce the same curve. For this reason, the notation of Equation (2.16) will be used in the following discussion with recognition of the fact that what is presented applies equally to Equation (2.26).

The form of the energy equation,

$$\left(1 + \frac{4}{3N}\right)\theta'' + \frac{Pr}{2} f\theta' = 0 ,$$

is much less complex than that of the momentum equation. The linearity also makes the possibilities for determining an analytic form of solution for θ more reasonable. The difficulty, however, arises in the fact that this equation is coupled to the momentum equation through f which has been determined to have no easily definable analytic form except in the region of the outer boundary of the mixing zone. Consequently, any analytic form obtained for θ would still be incomplete with respect to f. Once again, numerical solution appears to be the best approach. The only restriction involved here is that the value of f at all points of interest in the solution domain must be available before the solution can be specified.

The decision to seek a numerical solution for this equation gives rise to at least two other obstacles which must be overcome before success is attained. The first is that the boundary conditions for θ and θ' are specified at $-\infty$ and $+\infty$, points which have not, as yet, been defined from a numerical analysis standpoint. The second is that, unlike the momentum equation, no constraints have been specified for θ or θ' at $\eta = 0$. Thus it seems that there is no starting point for generating the solution curve. This statement is not entirely true, however, since knowledge of the behavior of the solution function at its extremes (+ ∞ and - ∞), and knowledge concerning the physical processes evident in the flow field does allow some intelligent analysis of the situation. The temperature distribution across the mixing zone, for example, must allow a smooth transition in the direction of - ∞ such that an asymptotic approach to the stagnation temperature, T_s, is attained. In other words, the absence of an adiabatic wall condition at - ∞ restricts the temperature difference, $T(\eta) - T_s$, and thus, the flux, θ', at - ∞ to asymptotically approach zero. Likewise, the freestream temperature, T_∞, is also asymptotically approached in the direction of + ∞, which requires that at + ∞, $T(\eta) - T_s$ is a maximum and θ' is again zero.

The character of the function at $\eta = 0$, though still not specified explicitly, must be such that none of the conditions above are violated. These restrictions in effect define a "window" in which a "set" of conditions may be specified for θ and θ' at $\eta = 0$ that allow the boundary conditions to be met. To illustrate, a chosen value for θ between 0 and 1 will possess a companion value of θ' which will satisfy the equation and its boundary conditions. The choice of θ may be considered somewhat arbitrary depending upon the problem parameters, but once θ is specified a unique value of θ' must be associated with it in order to effect a solution. The difficulty, as with $f''(0)$ in the momentum equation, lies in the correct choice of $\theta'(0)$. A method of eliminating much of the guesswork from this selection process has been developed by Nachtsheim and Swigert [13], and will be outlined in the next section.

C. Satisfaction of Asymptotic Boundary Conditions

The nature of the restrictions imposed on both the momentum and energy equations by the boundary conditions involved (i.e., f' and $\theta \rightarrow 0$ as $\eta \rightarrow -\infty$) indicates an asymptotic approach to a limiting value of zero for these functions. The method of Nachtsheim and Swigert provides a means for predicting the amount of error in an initial guess for the starting values used in numerical solution of differential equations which include asymptotic boundary conditions. Knowledge of the magnitude of this error then allows adjustment or correction of the initial guess to a degree commensurate with the limits of accuracy desired for the problem.

Application of this technique can be more clearly expressed, for purposes of discussion, by defining an arbitrary function $h(\eta)$ which is at least twice differentiable on the interval, $(0, \infty)$, with the conditions that

$$G(h,h') = \phi(\eta) \ ,$$

and

$$\lim_{\eta\to\infty} h(\eta) = 0 \ .$$

If the limiting condition is replaced with the condition that h = 0 at some specific value of η where the edge of the boundary layer interface occurs, then it can be related through the following:

$$h(\eta) = h_{edge} = 0 \text{ at } \eta = \eta_{edge} \ .$$

Since the ability to meet the condition is contingent on the value given to h' at zero, the boundary condition for h may be written as

$$h_{edge}(h'(0)) = 0 \ .$$

The value of $h'(0)$, if defined by the variable, x, indicates that a small change of Δx in x will change the value of h_{edge} by the amount

$$\frac{\partial h_{edge}}{\partial x} \Delta x \ .$$

Thus the correction to an approximation of the boundary condition for a given guess at the initial condition, $h'(0)$, can be given by

$$h_{edge} + \frac{\partial h_{edge}}{\partial x} \Delta x = 0 \ . \tag{3.6}$$

One can determine the magnitude of Δx required to produce the resulting perturbation in the value of h_{edge} provided the partial derivative of $h(\eta)$ with respect to x can be evaluated at η_{edge}. The evaluation can be performed by forming a perturbation equation, $G_x(h,h')$, from $G(h,h')$ by taking the derivative of G with respect to x and noting that

$$\frac{\partial h}{\partial x} = h_x, \text{ and } \frac{\partial h'}{\partial x} = h'_x \ .$$

This action provides a set of equations which may be solved for the value of Δx needed to correct the initial guess provided for x, or $h'(0)$. The starting conditions for $G_x(h,h')$ at $\eta = 0$ can be obtained from the conditions for $G(h,h')$ as follows:

$$\text{for } G(h,\ h');\ h(0) = 1$$
$$h'(0) = x \text{ (initial guess) ,}$$

and

$$\text{for } G_x(h,h');\ h_x(0) = \frac{\partial h(0)}{\partial x}$$
$$= \frac{\partial 1}{\partial x}$$
$$= 0$$

$$h'_x(0) = \frac{\partial h'(0)}{\partial x}$$

$$= \frac{\partial x}{\partial x}$$

$$= 1 \ .$$

These two equations can now be numerically integrated to the value of η_{edge} where the original boundary condition applies. The one remaining problem, of course, is that at this point in the solution sequence, the value of η_{edge} is not known. Help can be gotten to resolve this dilemma, however, by examining the behavior of the solution curve as η approaches ∞. First of all, the asymptotic approach to zero by h indicates that as η grows, the slope, h', of the function must also approach some limiting value. In this case, since the asymptote for h is the η axis, then the slope of the axis, which is zero, must be the limiting value for h'. Hence η_{edge} can be considered to be the point at which

$$h(\eta_{edge}) = 0 \ ,$$

and

$$h'(\eta_{edge}) = 0 \ .$$

Then the magnitude of Δx chosen must be appropriate to sufficiently correct h_{edge}. The result is that h_{edge} will allow the following two relations to be satisfied simultaneously:

$$h_{edge} + h_{x(edge)}\Delta x = 0 \tag{3.7a}$$

$$h'_{edge} + h'_{x(edge)}\Delta x = 0 \tag{3.7b}$$

The relations in Equation (3.7) can never be absolutely satisfied due to the mathematical limitations involved in actually reaching ∞. They can be satisfied, however, to some desired degree of accuracy such that

$$h_{edge} + h_{x(edge)}\Delta x = S_1$$

and

$$h'_{edge} + h'_{x(edge)}\Delta x = S_2 ,$$

where S_1 and S_2 are values arbitrarily close to zero. A least squares solution for Δx can be obtained for the above equations which will make the sum $S_1^2 + S_2^2$ as small as required. This can be accomplished by differentiating $S_1^2 + S_2^2$ with respect to Δx and equating the result to zero. To illustrate:

$$S_1^2 + S_2^2 = (h_{edge} + h_{x(edge)}\Delta x)^2 + (h'_{edge} + h'_{x(edge)}\Delta x)^2$$

$$\frac{\partial}{\partial \Delta x}(S_1^2 + S_2^2) = 2(h_{edge} + h_{x(edge)}\Delta x)h_{x(edge)} + 2(h'_{edge} + h'_{x(edge)}\Delta x)h'_{x(edge)}$$

$$2[h_{edge}\, h_{x(edge)} + h^2_{x(edge)}\Delta x + h'_{edge}\, h'_{x(edge)} + h'^2_{x(edge)}\Delta x] = 0$$

$$(h^2_{x(edge)} + h'^2_{x(edge)})\Delta x = - h_{edge}\, h_{x(edge)}$$
$$- h'_{edge}\, h'_{x(edge)}$$

$$\Delta x = - \frac{h_{edge}\, h_{x(edge)} - h'_{edge}\, h'_{x(edge)}}{h^2_{x(edge)} + h'^2_{x(edge)}} \,. \tag{3.8}$$

The relative degree of accuracy provided for the correction to the initial guess by Δx can be seen through examination of the deviations of h and h' from their asymptotic values at η_{edge}. The error, E, can be expressed as the sum of the squares of h_{edge} and h'_{edge} such that

$$E = h^2_{edge} + h'^2_{edge} \,. \tag{3.9}$$

Cases which involve asymptotes with values other than zero are also easily treated. For example, if the asymptotes for h and h' were 1 and 0 respectively, the error could be written as

$$E = (1 - h_{edge})^2 + h'^2_{edge} \,.$$

Attention can now be returned to application of the scheme described above to facilitate solution of the momentum and energy equations. The form of the momentum equation given in Equation (3.2) will be dealt with first. The perturbation equation is formed by taking the derivative with respect to x with the result that:

$$\frac{\partial}{\partial x}\,[2f''' + ff'' + R\eta f'^2] = 0$$

yields

$$2f_x''' + f_x f'' + ff_x'' + 2R\eta f' f_x' = 0.. \qquad (3.10)$$

The boundary conditions for Equation (3.2) restated for the interval, $(0,-\infty)$, are:

$$f(0) = 0,\ f'(0) = 1,\ f''(0) = x \text{ (initial guess)} \qquad (3.11a)$$

and

$$\lim_{\eta \to -\infty} f'(\eta) = 0,\ f''(\eta) = 0\ . \qquad (3.11b)$$

The starting conditions for the perturbation equation can now be derived from these as

$$f_x(0) = \frac{\partial f(0)}{\partial x} = 0\ ,\ f_x'(0) = \frac{\partial f'(0)}{\partial x} = 0\ ,$$

$$f_x''(0) = \frac{\partial f''(0)}{\partial x} = 1\ . \qquad (3.12)$$

Reference to Equations (3.7) and (3.8) show that for the solution curve, f', with slope, f'', the correction, Δx, to the starting condition $f''(0)$ is

$$\Delta x = \frac{-\ f' f_x' - f'' f_x''}{f_x'^2 + f_x''^2}\ . \qquad (3.13)$$

The error can be expressed as

$$E = f'^2 + f''^2\ . \qquad (3.14)$$

Now all the information necessary for a numerical solution to the momentum equation is assembled at this point. The only remaining task is that of conditioning the data and differential equation for insertion into the solution program. For solution in most algorithms, Equations (3.2) and (3.10) must be reduced to systems of simultaneous first order equations. This can be done through the substitution method by letting $f' = p$, and $p' = w$, respectively for Equation (3.2) to derive the following system:

$$p = f' \tag{3.15a}$$

$$w = p' \tag{3.15b}$$

$$w' = -\frac{1}{2}(fw + R\eta p^2) \ . \tag{3.15c}$$

A similar substitution for Equation (3.10) gives

$$p_x = f'_x \tag{3.16a}$$

$$w_x = p'_x \tag{3.16b}$$

$$w'_x = -\frac{1}{2}(f_x w_x + R\eta p_x^2) \ . \tag{3.16c}$$

The energy equation can be handled with the same ease as the momentum equation. The perturbation equation formed from Equation (2.16) is seen to be

$$\left(1 + \frac{4}{3N}\right)\theta''_x + \frac{\Pr f}{2}\,\theta'_x = 0 \ . \tag{3.17}$$

The initial conditions for the perturbation equation as derived from the initial conditions of Equation (2.16) are based on an assigned "set" of parameters at $\eta = 0$ for application to a solution on the interval, $(0, -\infty)$. If the value given for $\theta(0)$ is some number, a, the corresponding condition for $\theta'(0)$ can be expressed as $\theta'(0) = x$ (initial guess). The starting conditions for the perturbation equation, then, are

$$\theta_x(0) = \frac{\partial\theta(0)}{\partial x} = 0, \ \theta_x'(0) = \frac{\partial\theta'(0)}{\partial x} = 1 \ . \tag{3.18}$$

Reduction of Equations (2.16) and (3.17) to first order systems is accomplished as above by letting $\delta = \theta'$. The resulting two systems are

$$\delta = \theta' \tag{3.19a}$$

$$\delta' = -\frac{\left(\frac{\mathrm{Prf}}{2}\right)}{\left(1 + \frac{4}{3N}\right)}\delta \ , \tag{3.19b}$$

and

$$\delta_x = \theta_x' \tag{3.20a}$$

$$\delta_x' = -\frac{\left(\frac{\mathrm{Prf}}{2}\right)}{\left(1 + \frac{4}{3N}\right)}\delta_x \ . \tag{3.20b}$$

Equations (3.19) and (3.20), with their respective starting conditions, have now also been reduced to a form amenable to numerical solution once they have been conditioned for introduction into a suitable solution algorithm.

A number of solution algorithms for use with differential equations of the types mentioned above are in existence, some more suitable than others depending upon requirements for accuracy. They all must be modified somewhat, however, in order to fit the specific problem parameters outlined in this thesis. The particular algorithm selected, and the results obtained, will be discussed in the following paragraphs.

D. Results of the Solution Algorithm

The Runge-Kutta algorithm was chosen to solve the differential equations in question primarily because it is a stable algorithm and because the error inherent in numerical approximations using this scheme is generally well controlled. The specific form of the algorithm is one which utilizes Gill coefficients. Use of these coefficients in the algorithm allow somewhat better error control in moving from point to point across the solution interval. The algorithm has been incorporated into a computer program which is designed to compute the solution values for both the momentum and energy equations out to a point designated as η_{edge} where the corrections to the initial guesses for $f''(0)$ and $\theta'(0)$ are computed. The deviations of f' and θ from the asymptotic values are checked at η_{edge} and if the error is larger than a prescribed value, the magnitude of η_{edge} is increased. The new values for η_{edge} and the corrected initial guesses for

f'' and θ' are then used to re-solve the equations until the boundary conditions and error limits are met.

The integration is first performed in the negative η direction. Once this portion of the solution curve is completed, the corrected set of conditions at $\eta = 0$ is used to generate the solution curve in the positive η direction. Thus, the program automatically re-sets itself to integrate in the positive η direction until the conditions for $+\eta_{edge}$ are met. It should be recognized that the values for $\pm\eta_{edge}$ do not necessarily coincide for both the momentum and energy equations. This simply indicates that the velocity and thermal boundary layer thicknesses may differ. Solution of the energy equation, of course, requires that a value for the dimensionless stream function, f, be defined at every point where values of θ and θ' are needed. No problem exists so long as the velocity boundary layer is thicker than the thermal layer, but some need for caution arises if the thermal boundary layer is thicker. The reason is that the value of η_{edge} is considered to be ∞ for the purposes of numerical calculations. The theoretical meaning of this statement is that the function in question is assumed to have reached its limiting value and cannot be defined beyond η_{edge}. Hence, it would seem that no values for the stream function are available to use in solution of the energy equation beyond the value of η_{edge} for the velocity boundary layer. The fact is, however, that if one considers ∞ to have been reached, then the function value as well as those of its derivatives can be considered equal to the values of their respective asymptotes. Following this line of thought would dictate that the value of f at η_{edge} be used in the solution of the energy equation for any points beyond the edge of the velocity boundary layer.

The above reasoning is valid so long as the direction of integration is on the interval, $(0, -\infty)$, where the velocity profile must satisfy an asymptotic boundary condition. In the interval, $(0, +\infty)$, the absence of an asymptotic boundary condition (except for the case $R = 0$) is compensated for through use of the analytic solution to the condition $f''/f' = -R$. The analytic expression for the stream function obtained from this differential equation may be used to determine the value of f as far in the $+\eta$ direction as desired. This reasoning has been incorporated into the solution program so that its use may be generalized to any set of relationships which might exist between the velocity and thermal layers of the flow field under study.

Numerical results have been obtained for both velocity and temperature profiles in the curved free jet boundary based on the parameters listed in Table 1 below. The graph in Figure 2 shows the representative velocity profiles obtained for the five values of the curvature parameter, R, listed in Table 1. These curves show excellent agreement with the results reported in reference 5. They have been

TABLE 1

PARAMETERS FOR NUMERICAL SOLUTION OF THE MOMENTUM AND ENERGY EQUATIONS

Curvature Parameter, R	Conduction-To-Radiation Parameter, N	Prandtl Number, Pr
0.0	0.5	1.0
1.0×10^{-3}	1.0	
1.0×10^{-2}	∞	
4.0×10^{-2}		
1.0×10^{-1}		

Boundary Conditions for Momentum Equation

$\lim \eta \to -\infty$	$\eta = 0$	Large Positive η
$f'' = 0.0$	$f'' = 1.0$ (Initial Guess)	$\frac{f''}{f'} = -R$
$f' = 0.0$	$f' = 1.0$	
	$f = 0.0$	

Boundary Conditions for Energy Equation ($N = \infty$)

$\theta = 0.0$	$\theta = 0.586$	$\theta = 1.0$
$\theta' = 0.0$	$\theta' = -1.0$ (Initial Guess)	$\theta' = 0.0$

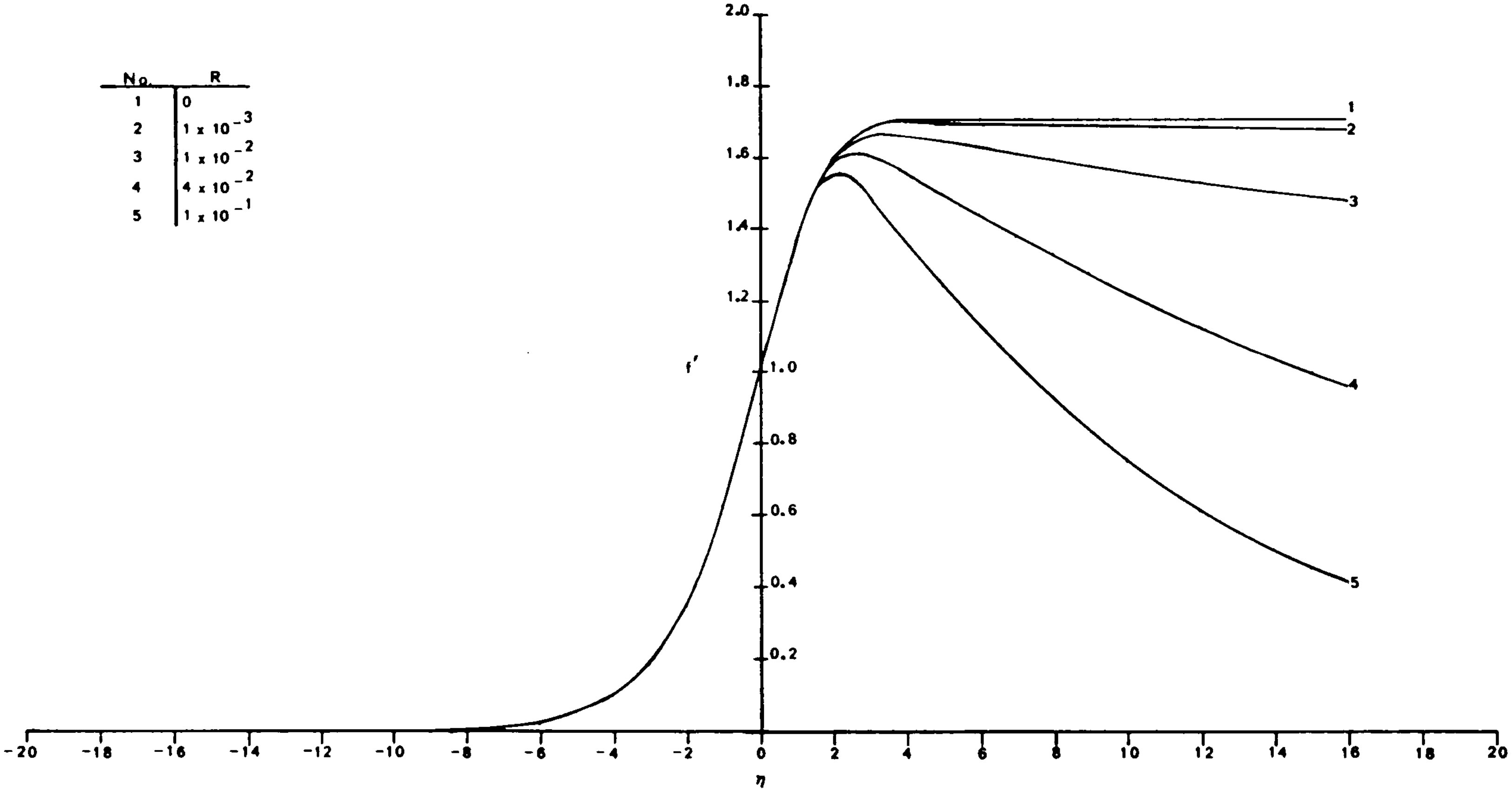

Figure 2. Velocity Profiles, $f'(\eta)$, for Variations in Curvature Parameter, R.

plotted here to a value of $\eta = 16.0$ to fully illustrate the effects of curvature on the outer portion of the velocity profile. The error bound utilized in the program to determine when boundary conditions were adequately met was set at 1.0×10^{-5} for both the momentum and energy equations.

The results in Table 2 provide solution values for boundary conditions on both equations. In all cases, the interval, $(0, -\infty)$, for the velocity profile terminates at $\eta = -8.500$, while the value of η where the boundary condition $f''/f' = -R$ is met decreases with increasing value of curvature parameter, R. The situation is somewhat different for the temperature profile, however. Limited examination of the data indicates that the extent of the thermal boundary layer grows in both the $+\eta$ and $-\eta$ directions with increasing curvature, but a detailed analysis will reveal the existence of more subtle trends. First of all, for the case where the conduction-to-radiation parameter, $N = \infty$, the corresponding condition for the flow field, as seen from Equation (2.16), is no contribution to the thermal boundary layer from radiative heat transfer. The chosen value, $\theta(0) = 0.586$, for the feasible set provides termination of the outer portion of the thermal boundary layer at $\eta = 4.1$. Extreme curvature ($R = 1 \times 10^{-1}$) required an increase in the value of $\theta(0)$ to 0.587 in order for a satisfactory solution to be obtained. This suggests

TABLE 2

COMPARISON OF VELOCITY AND THERMAL BOUNDARY LAYERS

R	Velocity Profile $-\eta_{edge}$	f'_{edge}	$+\eta_{B.C.}$*	$f'_{B.C.}$	$f''(0)$	Temperature Profile $-\eta_{edge}$	θ_{edge}	$+\eta_{edge}$	θ_{edge}	$\theta(0)$	$\theta'(0)$
	N = ∞			Thermal Radiation Effects Absent (Conduction Predominant)							
0.0	-8.500	0.81396 E-4	6.050	-0.17049 E+1	0.44477 E+0	- 8.600	0.49990 E-5	4.100	0.99868 E+0	0.586	0.26080 E+0
1.0×10^{-3}	-8.500	0.81565 E-4	4.937	0.16993 E+1	0.44499 E+0	- 8.600	0.50100 E-5	4.100	0.99863 E+0	0.586	0.26077 E+0
1.0×10^{-2}	-8.500	0.83086 E-4	4.100	0.16649 E+1	0.44697 E+0	- 8.600	0.51094 E-5	4.100	0.99823 E+0	0.586	0.26051 E+0
4.0×10^{-2}	-8.500	0.88126 E-4	3.583	0.15869 E+1	0.45345 E+0	- 8.600	0.54465 E-5	4.400	0.99751 E+0	0.586	0.25968 E+0
1.0×10^{-1}	-8.500	0.38858 E-4	3.282	0.14729 E+1	0.46590 E+0	- 8.500	0.70821 E-5	4.800	0.99700 E+0	0.587	0.25841 E+0
	N = 1.0			Radiation and Conduction Effects Approximately Equal							
0.0	-8.500	0.81396 E-4	6.050	0.17049 E+1	0.44477 E+0	-14.400	-0.26605 E-3	6.000	0.99745 E+0	0.631	0.15657 E+0
1.0×10^{-3}	-3.500	0.81565 E-4	4.937	0.16993 E+1	0.44499 E+0	-14.400	-0.26626 E-3	6.000	0.99757 E+0	0.631	0.15655 E+0
1.0×10^{-2}	-3.500	0.83086 E-4	4.100	0.16649 E+1	0.44697 E+0	-14.500	-0.26605 E-3	6.100	0.99856 E+0	0.631	0.15627 E+0
4.0×10^{-2}	-3.500	0.88126 E-4	3.583	0.15869 E+1	0.45345 E+0	-14.500	-0.26653 E-3	6.500	0.10014 E+1	0.631	0.15560 E+0
1.0×10^{-1}	-8.500	0.38858 E-4	3.282	0.14729 E+1	0.46590 E+0	-14.700	-0.26333 E-3	7.000	0.10013 E+1	0.629	0.15366 E+0
	N = 0.5			Thermal Radiation Effects Predominant**							
0.0	-8.500	0.81396 E-4	6.050	0.17047 E+1	0.44477 E+0	-20.200	-0.26659 E-3	7.900	0.99697 E+0	0.661	0.11610 E+0
1.0×10^{-3}	-8.500	0.81565 E-4	4.937	0.16993 E+1	0.44499 E+0	-20.200	-0.26678 E-3	7.400	0.99806 E+0	0.661	0.11608 E+0
						-20.200	-0.26637 E-3	7.900	0.99738 E+0	0.660	0.11590 E+0
1.0×10^{-2}	-8.500	0.83086 E-4	4.100	0.16649 E+1	0.44697 E+0	-20.300	-0.26314 E-3	7.700	0.10011 E+1	0.660	0.11568 E+0
						-20.200	-0.26583 E-3	14.800	0.99683 E+0	0.655	0.11477 E+0
4.0×10^{-2}	-8.500	0.88126 E-4	3.583	0.45345 E+1	0.45345 E+0	-20.300	-0.26637 E-3	8.600	0.10012 E+1	0.655	0.11412 E+0
						-20.300	-0.26438 E-3	10.800	0.99704 E+0	0.650	0.11329 E+0
1.0×10^{-1}	-8.500	0.38858 E-4	3.282	0.14729 E+1	0.46590 E+0	-20.500	-0.26480 E-3	9.500	0.10007 E+1	0.649	0.11186 E+0

*Location at which outer boundary condition $f''/f' = -R$ becomes valid.

**Additional values for temperature profile provided to show overlap conditions.

that severe curvature causes a rise in temperature along the major streamline of the curved flow field. The data for this value of N also shows a definite increase in the thickness of the boundary layer with increasing curvature.

When conduction and radiation effects in the boundary layer are almost equal ($N = 1$), the trend of increasing boundary layer thickness with increasing curvature is again evident. Significantly, however, the extent of the boundary layer in the direction of $-\eta$ is nearly 1.7 times that in the case for $N = \infty$. The case of extreme curvature produced an opposite effect in that the value of $\theta(0)$ had to be lowered from 0.631 to 0.629 to satisfy the requirements of the energy equation. This contradiction to the case for absent thermal radiation appears to indicate that severe curvature reduces the temperature along the major streamline when conduction and radiation contribute equally to the growth of the thermal boundary layer. This trend is supported through inspection of the values of θ_{edge} as R increases. Note that as R increases from 0.0 to 4.0×10^{-2}, the value of θ_{edge} increases from 0.99745 to 1.0014. It was found that using the value, $\theta(0) = 0.631$, for $R = 1.0 \times 10^{-1}$ produced an asymptotic value for θ_{edge} larger than 1.0014 and outside the error limits established for the computations. Thus, the reduction in $\theta(0)$ is indicated for two reasons. First, the theoretical limiting value of 1 for the temperature profile is violated, and second, the established accuracy limits cannot be met with the present value of $\theta(0)$. The value of $\theta(0)$ in the feasible set, then, must be adjusted in a direction where the boundary condition for $+\eta$ can be satisfied within accepted limits of accuracy.

A thermal boundary layer in which thermal radiation is predominant can be represented in the case where N is less than 1. Table 2 shows results for N = 0.5. Several sets of calculations were required to establish the trend illustrated for this case. This was due primarily to the fact that changes in curvature appeared to have a significantly greater effect on the extent of the boundary layer for this value of N. Thus, an overlapping technique was employed by determining the value of θ_{edge} for two slightly different values of $\theta(0)$ with each value of the curvature parameter between 0.0 and 1.0×10^{-1}. The resulting effect was that a value of $\theta(0)$ producing a solution for θ_{edge} in the low range of the error bound with a given curvature parameter provided a solution for θ_{edge} in the high range of the error bound for the next lower curvature parameter. This technique is permissible because the error, E, between the computed asymptotic value of θ_{edge} and its true value of 1 can be expressed as a function of the absolute value of some deviation, $\pm\Delta\theta$, on either side of 1. The implication, of course, is that given the range, $\pm\Delta\theta$, in which the solution requirements are satisfied, a corresponding range, $\Delta\theta(0)$, can be established for the feasible set which will provide these solutions.

Increases in curvature for $N = 0.5$ show an opposite effect on the boundary layer growth than do the cases for $N = \infty$ and $N = 1$. Although the extent of the thermal layer in the $-\eta$ direction is approximately 2.3 times that for the case of conduction only, the extent of the boundary is actually decreasing in the $+\eta$ direction. This decrease in the extent of the thermal layer is also accompanied by a decrease in the allowable temperature along the major streamline. The decrease in temperature along the major streamline agrees with the general trend established for equal effects of conduction and radiation, but the resultant effect of curvature appears to be much more pronounced. It might be well at this point to remark, by reference again to Figure 2 on page 54, that for approaches to severe curvature, the value of f' begins to fall off sharply once the curvature constraint for the boundary condition is satisfied. This indicates, of course, that the velocity in the flow field begins to decrease for values of η beyond the point where the curvature boundary condition is met. One might infer, then, that some connection exists between the significant velocity change and the significant change in thermal boundary layer thickness for severe curvature.

Shown in Figure 3 is a graphic comparison of temperature profiles for all three values of N reported in the tabulated data. The plots in the figure, based on detailed numerical results obtained for each curvature value, indicate that the shape of the profiles is essentially unchanged with the exception of extension or reduction of the boundary layer thickness.

More insight into the nature of heat transfer in the curved flow field can be gained through an examination of how the heat flux, q, is affected by curvature. In general terms, the heat flux is defined through the expression

$$q = - K \frac{\partial T}{\partial y} .$$

For the case where both conduction and radiation are evident in the boundary layer, the heat flux can be expressed through the relation

$$q = q_c + q_r ,$$

where q_c represents the flux due to conduction and q_r is the flux due to radiative interactions. In terms of fully expanded definitions,

$$q = - K \frac{\partial T}{\partial y} - \frac{4\lambda^2\sigma}{3\kappa} \frac{\partial T^4}{\partial y} .$$

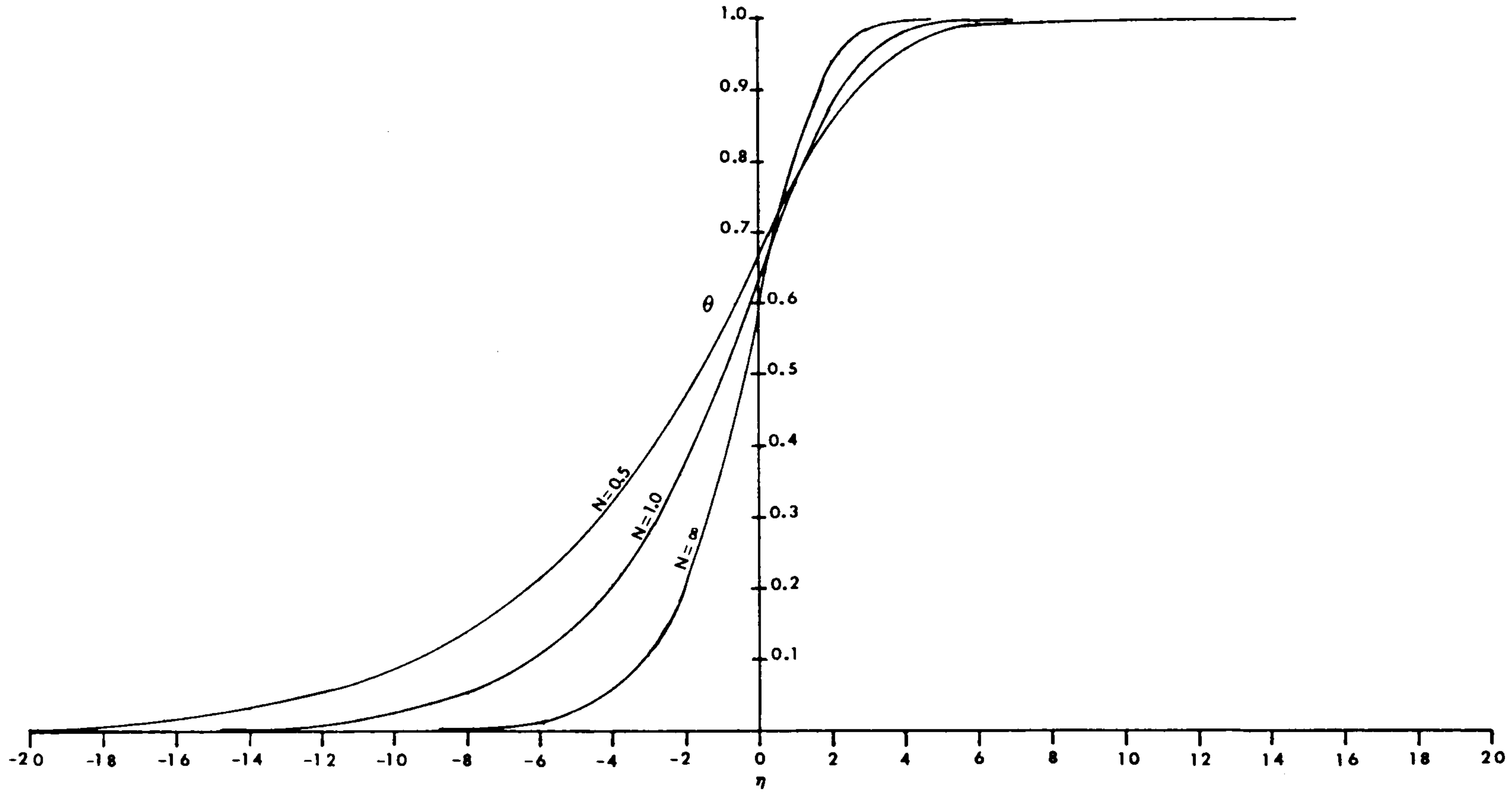

Figure 3. Temperature Profiles for Varying Curvature Parameter, R. (Refer to Table 2, page 56, for related values of $\pm\,\theta_{edge}$ and R.)

The point of interest for examining changes in heat flux is centered around the major streamline. This is primarily due to the fact that it is this reference which has been utilized as the starting point of the solution. Under most circumstances, when a boundary condition involving an adiabatic wall constraint is involved in determinations of boundary layer thickness, the flux at the wall is important. In this case, since there is no wall involved, the flux at the major streamline will provide some degree of understanding of the mechanisms of heat transfer across the boundary layer. The rate of heat transfer at the major streamline, defined as q_m, then can be specified as

$$q_m = - K \left(\frac{\partial T}{\partial y}\right)_{y = 0} - \frac{4\lambda^2\sigma}{3\kappa}\left(\frac{\partial T^4}{\partial y}\right)_{y = 0} .$$

This can further be expressed as follows if the temperature linearizing approximation is again employed:

$$q_m = - \left(K + \frac{16\lambda^2\sigma T_\infty^3}{3\kappa}\right)\left(\frac{\partial T}{\partial y}\right)_{y = 0} .$$

The dimensionless transformation used in Chapter II can also be employed to arrive at a dimensionless expression for the heat flux. Recall that in terms of transformed variables,

$$\frac{\partial T}{\partial y} = T' \ (U_1/\nu x)^{1/2}$$

and

$$N = \frac{\kappa K}{4\lambda^2 \sigma T_\infty^3} \ .$$

Thus

$$q_m = - K(U_1/\nu x)^{1/2}\left(1 + \frac{4}{3N}\right)\left(\frac{\partial T}{\partial \eta}\right)_{\eta = 0} \ ,$$

and again using the dimensionless θ,

$$q_m = - K(U_1/\nu x)^{1/2}\left(1 + \frac{4}{3N}\right)\theta'(0)\,(T_\infty - T_s) \ .$$

Simplification yields

$$\frac{q_m}{K(T_s - T_\infty)}\left(\frac{\nu x}{U_1}\right)^{1/2} = + \left(1 + \frac{4}{3N}\right)\theta'(0)$$

where multiplication of the left side by x^2/x^2 reduces the equation to

$$\frac{q_m x}{K(T_s - T_\infty)}\left(\frac{\nu}{U_1 x}\right)^{1/2} = \left(1 + \frac{4}{3N}\right)\theta'(0) \ .$$

The quantity $\frac{q_m x}{K(T_s - T_\infty)}$ is defined as the Nusselt number, Nu, while $\left(\frac{\nu}{U_1 x}\right)^{1/2}$ is the reciprocal of the square root of the Reynolds number, Re, so that

$$\frac{Nu}{\sqrt{Re}} = \left(1 + \frac{4}{3N}\right)\theta'(0) \ .$$

The above equation illustrates that the heat flux across the major streamline can be expressed as the ratio of two dimensionless numbers as shown. The value of $\theta'(0)$ can be taken directly from Table 2 on page 56 and the quantity $\left(1 + \frac{4}{3N}\right)$ can be determined for the values of N given. The plots in Figure 4 show changes in the ratio of Nusselt number to square root of the Reynolds number for variations in the curvature parameter with values of $N = \infty$, 1, and 0.5. Results from the graph indicate that curvature affects the heat flux across the major streamline very little. In fact, the curve for $N = \infty$ is nearly flat, and the curves for $N = 1$ and 0.5 also show a very nearly linear relationship except in the region of curvature range between 10^{-2} and 10^{-1}. Departure from linearity is most noticeable in this region for the $N = 0.5$ curve where the value of the heat flux is observed to decrease with the approach to severe curvature limits.

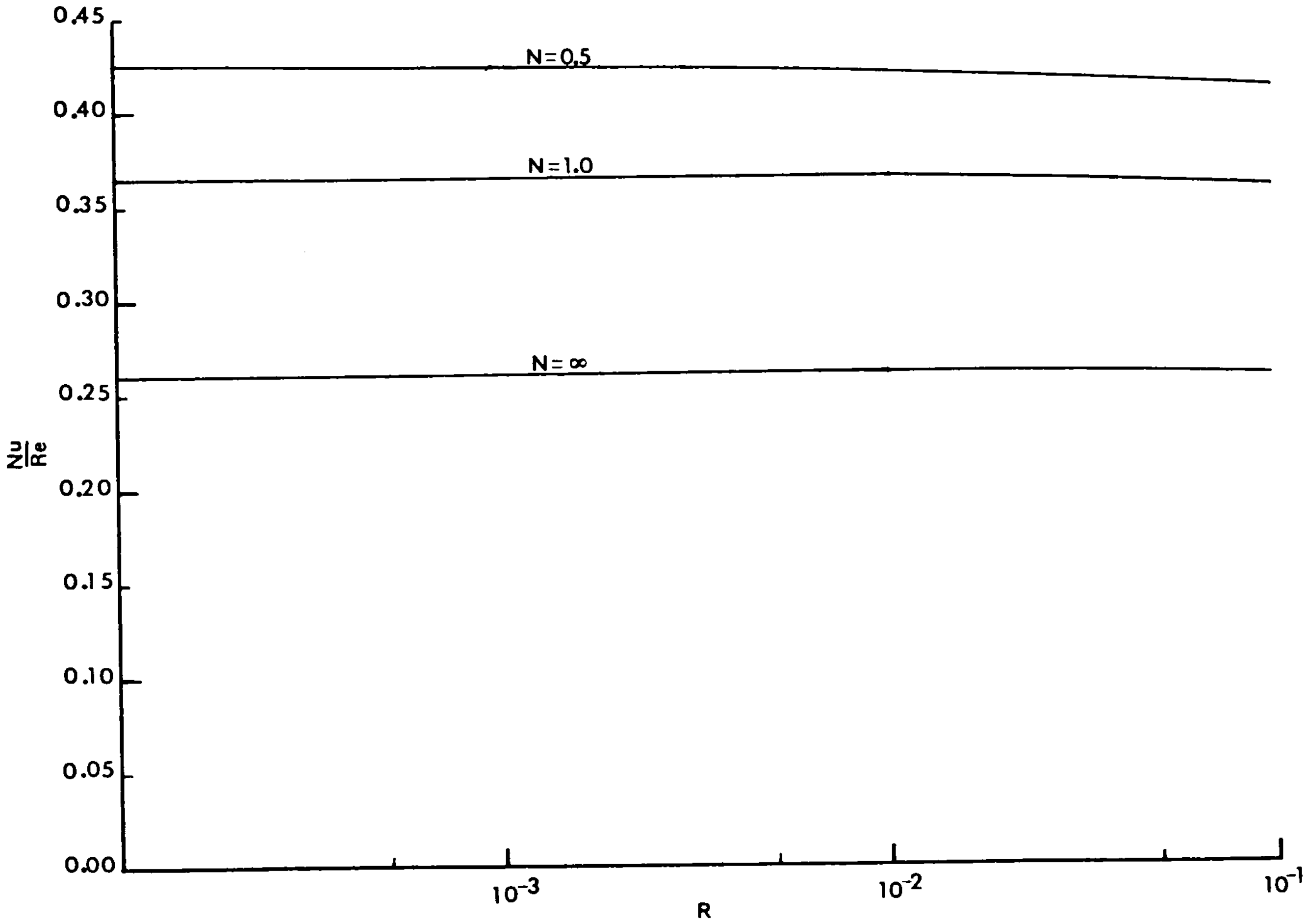

Figure 4. Variation of $Nu/\sqrt{Re}$ with Curvature Parameter, R.

CHAPTER IV

CONCLUSIONS AND RECOMMENDATIONS

The results of this study provide a great deal of information which can be utilized to formulate certain conclusions relative to the role of thermal radiation in heat transfer across the curved free jet boundary. The sake of consistency, however, dictates that a brief recount of the parameters constraining the research is in order before the discussion continues.

The problem examined was that of ascertaining the effects of variations in curvature on the temperature profile and on heat transfer characteristics in the mixing region surrounding the boundaries of free jet-type flows. Particular interest was directed at how these effects changed based on differing degrees of heat transfer due to thermal radiation. Solution of the boundary layer equations used in the problem analysis was effected through employment of a similarity transformation which produced ordinary differential forms of the momentum and energy equations. Solution of the energy equation was simplified first of all, by use of the Rosseland approximation for optically thick thermal radiation, and secondly by application of a linearization technique in order to remove the nonlinear dependence upon temperature. The momentum and energy equations were numerically solved by using a perturbation method designed to provide corrections to initial guesses for the slope of the velocity and temperature profile curves respectively. Results have been presented for three values of the conduction-to-radiation parameter to include $N = \infty$, 1.0, and 0.5, with values of the curvature parameter R ranging from 0.0 to 1.0×10^{-1}.

Study of the temperature profiles and supporting data brings out the following conclusions:

1. The general tendency of the thermal boundary layer is to thicken with increasing contributions from thermal radiation.
2. When heat transfer by conduction is predominant, the depth of the thermal boundary layer increases, primarily in the direction of the freestream, with an accompanying rise in temperature along the major streamline, as curvature increases to severe limits.
3. When heat transfer by thermal radiation is predominant, the depth of the thermal boundary layer decreases, primarily in the direction of the freestream, with an accompanying reduction in temperature along the major streamline, as curvature increases to severe limits.
4. With the major streamline as a reference point in the flow, the temperature gradient at this point is

found to decrease as radiation effects become more predominant, while the heat flux across the streamline increases. At the same time, increase in the curvature of the flow field for any given magnitude of radiative participation produces a reduction in both the temperature gradient and the heat flux at the major streamline.

The results concerning the effects of radiation on the thermal boundary layer growth are in agreement with work done by Viskanta and Grosh, and are in conformance with the generally accepted theories set forth in the literature. The results concerning the effects of curvature can be explained in part through some discussion of the nature of the transport processes evident in the flow. In the case where conduction is predominant, for example, the velocity profile decreases more sharply in the direction of the freestream as more severe curvature constraints are placed on the system. The indication is that the fluid begins to move more slowly as the point of curvature domination in the flow is passed. The slower moving fluid will have an adverse effect on the convective transfers which are occurring in the direction of the stagnation region with the result that the heat transfer rate across the major streamline is decreased, thus increasing the boundary layer depth. If the curvature constraints on the system become severe enough, reverse flow conditions can become evident, causing formation of a cavity by wall attachment of the jet somewhere in the stagnation region. When this takes place, enhanced mixing of the two fluid layers can occur. Such a phenomenon would, in effect, raise the stagnation temperature observed from the vantage point of the major streamline. This action may be responsible for the noted rise in temperature at the major streamline for the case of pure conduction.

Predominant radiation presents an opposite effect from that discussed above for predominant conduction. This is partly due to the highly nonlinear dependence upon temperature of the heat flux across the major streamline. The dependence, of course, is felt through influence of the reciprocal relationship between the conduction-to-radiation parameter, N, and the temperature gradient, θ', in the expression for the total heat flux. Inherent in the optically thick approximation also is an underestimation of the radiant flux at the boundary [9, 12], so that part of the explanation for the variations in $\theta(0)$ for the case of predominant radiation might lie in the error introduced in this manner. The subsequent reductions of temperature gradient and heat flux across the major streamline can once again be explained through the influence of curvature on convective transfers. The reduction of fluid velocity from the point of curvature domination in the flow field reduces the capability for fluid particles to interact with one another. The restrictions placed on the radiant heat flux through the optically thick approximation would require that decreases in mobility of the fluid particles lessen the extent to which absorption and emission of thermal radiation by individual particles could take place. The result would be a decrease in the extent of the thermal boundary layer. The limits of severe curvature and reverse flow might not be sufficient to cancel this trend due to the fact that any enhanced mixing of the fluid streams might occur beyond the boundary in the flow field where the stagnation temperature, T_s, is reached. The underestimation of flux at this boundary could possibly reduce any trend reversing effects of enhanced mixing to negligible levels.

Future research should concentrate on obtaining more exact expressions for the contributions due to thermal radiation. The restriction to optically thick radiation is somewhat of an oversimplification if precise approximations for heat transfer across the thermal boundary layer are required. It is adequate, however, to establish general ideas about the behavior of the energy transport processes at work in the curved jet boundary. Additional refinements can be realized also through consideration of the nonlinear dependence of the energy balance on the temperature. The temperature linearization technique utilized in this study allows a first order approximation to be made, but it has been illustrated through the results that strong dependence on nonlinear characteristics of the temperature function is evident. Therefore, it would be of interest to investigate the effect of including a nonlinear expression for the temperature gradient in the energy equation in order to compare the results with those presented here.

LIST OF REFERENCES

LIST OF REFERENCES

1. Schlichting, H., Boundary Layer Theory, 4th ed., McGraw-Hill, New York, 1960.

2. White, H. M., Viscous Fluid Flows, 1st ed., McGraw-Hill, New York, 1974.

3. Sawyer, R. A., "The Flow Due to a Two-Dimensional Jet Issuing Parallel to a Flat Plate," Journal of Fluid Mechanics, Vol. 9, 1960, pp. 543-561.

4. Sawyer, R. A., "Two Dimensional Reattaching Jet Flows Including the Effects of Curvature on Entrainment," Journal of Fluid Mechanics, Vol. 17, 1963, pp. 481-498.

5. Williams, J. C., Cheng, E. H., and Kim, K. H., "Curvature Effects in the Laminar and Turbulent Freejet Boundary," AIAA Journal, Vol. 9, No. 4, April 1971, pp. 733-736.

6. Murphy, J. S., "Some Effects of Surface Curvature on Laminar Boundary Layer Flow," Journal of the Aeronautical Sciences, Vol. 20, No. 5, May 1953, pp. 338-344.

7. Reichardt, H., "Momentum and Heat Exchange in Free Turbulence," Journal of Applied Mathematics and Mechanics, Vol. 24, No. 5, June 1944.

8. Kestin, J., and Richardson, P. D., "Heat Transfer Across Turbulent, Incompressible Boundary Layers," International Journal of Heat and Mass Transfer, Vol. 6, 1963, pp. 147-189.

9. Viskanta, R., and Grosh, R. J., "Boundary Layer in Thermal Radiation Absorbing and Emitting Media," International Journal of Heat and Mass Transfer, Vol. 5, 1962, pp. 795-806.

10. Bloom, N., "Remarks on Thermal Characteristics of Boundary Layers," Journal of the Aeronautical Sciences, May 1953, pp. 363-364.

11. Smith, J. W., "Effect of Gas Radiation in the Boundary Layer on Aerodynamic Heat Transfer," Journal of the Aeronautical Sciences, August 1953, pp. 578-580.

12. Sparrow, E. M., and Cess, R. D., Radiation Heat Transfer, 1st ed., Brooks/Cole Publishing, Belmont, California, 1966.

13. Nachtsheim, P. R., and Swigert, Paul, "Satisfaction of Asymptotic Boundary Conditions in Numerical Solution of Systems of Non-linear Equations of Boundary Layer Type," NASA Technical Note D-3004, National Aeronautics and Space Administration, 1965.

14. Burden, R. L., Faires, J. D., and Reynolds, A. C., Numerical Analysis, 1st ed., Prindle Weber and Schmidt, Boston, Mass., 1978.

APPENDIX

APPENDIX

The following program was used to generate solution data discussed in the thesis.

```
      IMPLICIT REAL*8(A-H,O-Z),INTEGER(I-N)
      DIMENSION YS(20),Y(20),Q(20),STR(5)
      DIMENSION ETA(600),PRIM1(600),PRIM2(600),PRIM3(600)
      DIMENSION CHECK(600),BIN(20),B1(600),B2(600),
     1B3(600)
      DIMENSION THETA1(600),THETA2(600)
      DIMENSION STORE1(600),STORE2(600),AXIS(600)
      DIMENSION POINT(20),G1(20),G2(20),G3(20),V1(20),
     1V2(20),V3(20)
      COMMON R,CR,PR
C
C INTEGRATION OF MOMENTUM EQUATION WITH CURVATURE "R".
C
      WRITE (16,102)
  102 FORMAT ('*** INTEGRATED RESULTS FOR MOMENTUM ***')
      DO 501 K=2,2
      ZK=K
      R=0.0D0
      PR=1.0D0
      CR=10.0D0
      DO 500 I=3,3
         EMAX=0.1D-4
         DZMAX=0.1D+01
         N1=10
         N2=3
         N3=1
         W=1.0D0
         STR(1)=0.0D0
         STR(2)=0.0D0
         STR(3)=0.0D0
         NDNF=1
         DX=0.05D0
         NDXW=1
         NF=NDNF
         Z=1.0D0
         ISFW=10
    1    XS=0.0D0
         YS(1)=0.0D0
         YS(2)=1.0D0
         YS(3)=Z
         YS(4)=0.0D0
         YS(5)=0.0D0
         YS(6)=1.0D0
         YS(7)=0.630D0
         YS(8)=-Z
         YS(9)=0.0D0
         YS(10)=1.0D0
         BIN(1)=0.0D0
         BIN(2)=0.0D0
         BIN(3)=0.0D0
  200    WRITE (16,201) XS,YS(1),YS(2),YS(3),YS(4),YS(5),
     1   YS(6)
  201    FORMAT (F7.3,6D16.8)
   34    ISR=0
         INF=1
```

```
      STEP=-DX
    3 CALL RNKTGL(N1,N2,N3,W,BIN,STR,ISR,XS,STEP,DX,
     1 NDXW,YS,XFC,Y,Q)
      IF(ISFW-5) 45,45,300
  300 ETA(INF)=XFC
      PRIM1(INF)=Y(1)
      PRIM2(INF)=Y(2)
      PRIM3(INF)=Y(3)
   45 IF(INF-NF) 4,5,5
    4 INF=INF+1
      ISR=ISR+1
      GO TO 3
    5 DZ=(-Y(2)*Y(5)-Y(3)*Y(6))/(Y(5)**2+Y(6)**2)
      E=Y(2)**2+Y(3)**2
      Z=Z+DZ
      IF(DABS(DZ/Z).GT.DZMAX) GO TO 1
      IF(E-EMAX) 13,14,14
   14 NF=NF+NDNF
      GO TO 1
   13 IF(ISFW-5) 401,401,402
  401 ISFW=ISFW+10
      Z=Z-DZ
      GO TO 1
  402 WRITE (16,203) E
  203 FORMAT (3H E=,D16.8)
  500 CONTINUE
  501 CONTINUE
      TEMP1=PRIM1(1)
      PRIM1(1)=YS(1)
      TEMP3=PRIM2(1)
      PRIM2(1)=YS(2)
      TEMP5=PRIM3(1)
      PRIM3(1)=YS(3)
      TEMP7=ETA(1)
      ETA(1)=XS
      DO 510 IA=1,INF
        IB=IA+1
        TEMP2=PRIM1(IB)
        PRIM1(IB)=TEMP1
        TEMP1=TEMP2
        TEMP4=PRIM2(IB)
        PRIM2(IB)=TEMP3
        TEMP3=TEMP4
        TEMP6=PRIM3(IB)
        PRIM3(IB)=TEMP5
        TEMP5=TEMP6
        TEMP8=ETA(IB)
        ETA(IB)=TEMP7
        TEMP7=TEMP8
  510 CONTINUE
      INF=INF+1
      DO 700 I=1,INF,2
        WRITE (16,205) ETA(I),PRIM1(I),PRIM2(I),PRIM3(I)
  205   FORMAT (F7.3,3D16.8)
  700 CONTINUE
```

```
      WRITE (16,210)
  210 FORMAT (/,10X,'****VALUES OF ETA PLUS****',/)
      WRITE (16,201) XS,YS(1),YS(2),YS(3),YS(4),YS(5),
     1YS(6)
      STORE2(1)=YS(1)
      AXIS(1)=XS
      J=2
      L=INF+1
      NDXW=1
      ISR=0
      STEP=DX
      YS(3)=-YS(3)
  705 CALL RNKTGL(N1,N2,N3,W,BIN,STR,ISR,XS,STEP,DX,
     1NDXW,YS,XFC,Y,Q)
      ETA(L)=XFC
      PRIM1(L)=Y(1)
      PRIM2(L)=Y(2)
      PRIM3(L)=Y(3)
      B1(L)=Q(1)
      B2(L)=Q(2)
      B3(L)=Q(3)
      AXIS(J)=XFC
      STORE2(J)=Y(1)
      CHECK(L)=PRIM3(L)+R*PRIM2(L)
      IF(DABS(CHECK(L)).LE.EMAX) GO TO 710
      IF(L.EQ.600) GO TO 1380
      IF(CHECK(L).LT.0.0D0) GO TO 888
      GO TO 706
  888 LBC=L-1
      XS=ETA(LBC)
      YS(1)=PRIM1(LBC)
      YS(2)=PRIM2(LBC)
      YS(3)=PRIM3(LBC)
      BIN(1)=B1(LBC)
      BIN(2)=B2(LBC)
      BIN(3)=B3(LBC)
      DX=0.5D0*DX
      STEP=DX
      W=-1.0D0
      ISR=0
      LBR=1
  889 CALL RNKTGL(N1,N2,N3,W,BIN,STR,ISR,XS,STEP,DX,
     1NDXW,YS,XFC,Y,Q)
      POINT(LBR)=XFC
      G1(LBR)=Q(1)
      G2(LBR)=Q(2)
      G3(LBR)=Q(3)
      V1(LBR)=Y(1)
      V2(LBR)=Y(2)
      V3(LBR)=Y(3)
      BC=V3(LBR)+R*V2(LBR)
      IF(DABS(BC).LE.EMAX) GO TO 712
      IF(BC.LT.0.0D0) GO TO 855
      GO TO 857
  855 IF(LBR.EQ.1) GO TO 888
```

```
      LBR=LBR-1
      DX=0.5D0*DX
      STEP=DX
      XS=POINT(LBR)
      YS(1)=V1(LBR)
      YS(2)=V2(LBR)
      YS(3)=V3(LBR)
      BIN(1)=G1(LBR)
      BIN(2)=G2(LBR)
      BIN(3)=G3(LBR)
      LBR=LBR+1
      ISR=0
      GO TO 889
  857 ISR=ISR+1
      LBR=LBR+1
      GO TO 889
  706 ISR=ISR+1
      L=L+1
      J=J+1
      GO TO 705
  710 LBR=1
      V1(LBR)=PRIM1(L)
      V2(LBR)=PRIM2(L)
      V3(LBR)=PRIM3(L)
      POINT(LBR)=ETA(L)
  712 DX=0.05D0
      STEP=DX
      IF(R) 810,800,810
  800 BETA1=V2(LBR)
      BETA2=V1(LBR)-BETA1*POINT(LBR)
      IF(DABS(CHECK(L)).LE.EMAX) GO TO 860
      GO TO 820
  810 BETA1=V2(LBR)*DEXP(R*POINT(LBR))
      BETA2=V1(LBR)-BETA1*DEXP(-R*POINT(LBR))
      IF(DABS(CHECK(L)).LE.EMAX) GO TO 860
  820 IF(R) 840,830,840
  830 PRIM1(L)=BETA1*ETA(L)+BETA2
      PRIM2(L)=BETA1
      PRIM3(L)=0.0D0
      STORE2(J)=PRIM1(L)
      GO TO 850
  840 PRIM1(L)=BETA2+BETA1*DEXP(-R*ETA(L))
      PRIM2(L)=BETA1*DEXP(-R*ETA(L))
      PRIM3(L)=-R*PRIM2(L)
      STORE2(J)=PRIM1(L)
  850 IF(ETA(L)-16.0D0) 860,870,870
  860 LAST=L
      L=L+1
      J=J+1
      ETA(L)=ETA(LAST)+STEP
      AXIS(J)=ETA(L)
      GO TO 820
  870 J=J+1
      DO 815 I=J,300
        JB=I-1
```

```
      AXIS(I)=AXIS(JB)+STEP
      IF(R) 819,817,819
817   STORE2(I)=BETA2+BETA1*AXIS(I)
      GO TO 815
819   STORE2(I)=BETA2+BETA1*DEXP(-R*AXIS(I))
815 CONTINUE
    WRITE(16,219) POINT(LBR),V2(LBR)
219 FORMAT(/,' BDY. COND. MET:ETA= ',F8.4,3X,'F PRIME='
   1,D16.8)
    INIT=INF+1
    DO 715 I=INIT,L,2
    WRITE (16,206) ETA(I),PRIM1(I),PRIM2(I),PRIM3(I)
206 FORMAT(1X,F7.4,3D16.8)
715 CONTINUE
    WRITE(16,207)
207 FORMAT(/,10X,'****TEMPERATURE PROFILE****',/)
    DO 890 I=1,300
      IF(I.GE.INF) GO TO 891
      STORE1(I)=PRIM1(I)
      GO TO 890
891   STORE1(I)=PRIM1(INF)
890 CONTINUE
    INFT=INF/2
    DO 901 I=2,2
    DO 900 K=3,3
      N1=10
      N2=3
      N3=7
      W=1.0D0
      DX=0.1D0
      STEP=-DX
      NDNF=1
      NDXW=1
      NF=INFT
      Z=-1.0D0
      ISFW=10
902   YS(8)=Z
      XS=0.0D0
      BIN(1)=0.0D0
      BIN(2)=0.0D0
      BIN(3)=0.0D0
903   WRITE(16,904) XS,YS(7),YS(8),YS(9),YS(10)
904   FORMAT(F7.3,4D16.8)
934   ISR=0
      IT=1
      JUMP=0
933   L1=IT+JUMP
      L2=IT+(JUMP+1)
      L3=IT+(JUMP+2)
      STR(1)=STORE1(L1)
      STR(2)=STORE1(L2)
      STR(3)=STORE1(L3)
      J=IT
      CALL RNKTGL(N1,N2,N3,W,BIN,STR,ISR,XS,STEP,DX,
     1 NDXW,YS,XFC,Y,Q)
```

```
      IF(ISFW-5) 945,945,950
950   ETA(IT)=XFC
      THETA1(IT)=Y(7)
      THETA2(IT)=Y(8)
945   IF(IT-NF) 999,1000,1000
999   IT=IT+1
      ISR=ISR+1
      JUMP=JUMP+1
      GO TO 933
1000  DZ=(-Y(7)*Y(9)-Y(8)*Y(10))/(Y(9)**2+Y(10)**2)
      E=Y(7)**2+Y(8)**2
      Z=Z+DZ
      IF(DABS(DZ/Z).GT.DZMAX) GO TO 902
      IF(E-EMAX) 943,944,944
944   NF=NF+NDNF
      GO TO 902
943   IF(ISFW-5) 921,921,922
921   ISFW=ISFW+10
      Z=Z-DZ
      GO TO 902
922   WRITE(16,905) E
905   FORMAT(3H E=,D16.8)
900 CONTINUE
901 CONTINUE
    DO 1200 I=1,IT
      WRITE(16,906) ETA(I),THETA1(I),THETA2(I)
906   FORMAT(1X,F7.3,2D16.8)
1200 CONTINUE
    WRITE(16,210)
    ISR=0
    DX=2.0D0*(AXIS(2)-AXIS(1))
    STEP=DX
    YS(8)=-YS(8)
    IT=IT+1
    IP=IT
    JUMP=0
    IQ=1
1300 L1=IQ+JUMP
    L2=IQ+(JUMP+1)
    L3=IQ+(JUMP+2)
    STR(1)=STORE2(L1)
    STR(2)=STORE2(L2)
    STR(3)=STORE2(L3)
    CALL RMKTGL(N1,N2,N3,W,BIN,STR,ISR,XS,STEP,DX,
   1NDXW,YS,XFC,Y,Q)
    ETA(IT)=XFC
    THETA1(IT)=Y(7)
    THETA2(IT)=Y(8)
    DIFF=1.0D0-THETA1(IT)
    E=DIFF**2+THETA2(IT)**2
    IF(E.LE.EMAX) GO TO 1386
    IF(THETA1(IT).GE.1.0D0) GO TO 1350
    IF(IT.GE.300) GO TO 1385
    IT=IT+1
    ISR=ISR+1
```

```
      JUMP=JUMP+1
      IQ=IQ+1
      GO TO 1300
 1350 DO 1370 I=IP,IT
        WRITE(16,1360) ETA(I),THETA1(I),THETA2(I)
 1360   FORMAT(F8.4,2D16.8)
 1370 CONTINUE
      GO TO 1390
 1380 WRITE(16,1400)
 1400 FORMAT(' VELOCITY MATRIX FULL FOR ETA PLUS ')
      GO TO 1390
 1385 WRITE(16,1410)
 1410 FORMAT(' TEMPERATURE MATRIX FULL FOR ETA PLUS ')
      GO TO 1350
 1386 WRITE(16,1412) ETA(IT)
 1412 FORMAT(/,' ASYMPTOTE REACHED AT ',F8.4,/)
      GO TO 1350
 1390 STOP
      END
      SUBROUTINE RNKTGL(N1,N2,N3,W,BIN,STR,ISR,XS,STEP,DX
     1,NDXW,YS,XFC,Y,Q)
      IMPLICIT REAL*8(A-H,O-Z),INTEGER(I-N)
      DIMENSION YS(20),F(20),Y(20),Q(20)
      DIMENSION BIN(20)
      DIMENSION STR(5)
      COMMON R,CR,PR
      A1=0.5D0
      A2=0.1D+01-DSQRT(0.5D0)
      A3=0.1D+01+DSQRT(0.5D0)
      A4=0.1D+01/0.6D+01
      COUNT=-1.0D0
      IF(N3.EQ.7) COUNT=1.0D0
      IF(W) 3,6,6
    6 IF(ISR) 1,1,60
    1 X=XS
      DO 2 I=N3,N1
        Y(I)=YS(I)
        Q(I)=0.0
    2 CONTINUE
      N=N1
      GO TO 60
    3 IF(ISR) 50,50,60
   50 X=XS
      DO 4 I=N3,N2
        Y(I)=YS(I)
        Q(I)=BIN(I)
    4 CONTINUE
      N=N2
   60 IDX=1
    5 PSI=STR(1)
      CALL FNLIST(X,Y,COUNT,PSI,F)
      DO 10 I=N3,N
        DK1=DX*F(I)
        Y(I)=Y(I)+A1*(DK1-0.2D+01*Q(I))
        Q(I)=Q(I)+0.3D+01*A1*(DK1-0.2D+01*Q(I))-A1*DK1
```

```
10 CONTINUE
   X=X+0.5D0*STEP
   PSI=STR(2)
   CALL FNLIST(X,Y,COUNT,PSI,F)
   DO 20 I=N3,M
     DK2=DX*F(I)
     Y(I)=Y(I)+A2*(DK2-Q(I))
     Q(I)=Q(I)+0.3D+01*A2*(DK2-Q(I))-A2*DK2
20 CONTINUE
   CALL FNLIST(X,Y,COUNT,PSI,F)
   DO 30 I=N3,M
     DK3=DX*F(I)
     Y(I)=Y(I)+A3*(DK3-Q(I))
     Q(I)=Q(I)+0.3D+01*A3*(DK3-Q(I))-A3*DK3
30 CONTINUE
   X=X+0.5D0*STEP
   PSI=STR(3)
   CALL FNLIST(X,Y,COUNT,PSI,F)
   DO 40 I=N3,M
     DK4=DX*F(I)
     Y(I)=Y(I)+A4*(DK4-0.2D+01*Q(I))
     Q(I)=Q(I)+0.3D+01*A4*(DK4-0.2D+01*Q(I))-A4*DK4
40 CONTINUE
   IF(IDX-NDXW) 41,42,42
41 IDX=IDX+1
   GO TO 5
42 XFC=X
   RETURN
   END
   SUBROUTINE FNLIST(X,Y,COUNT,PSI,F)
   IMPLICIT REAL*8(A-H,O-Z),INTEGER(I-N)
   DIMENSION Y(20),F(20)
   COMMON R,CR,PR
   IF(COUNT) 10,10,20
10 F(1)=Y(2)
   F(2)=Y(3)
   F(3)=-0.5D0*Y(1)*Y(3)-0.5D0*X*R*Y(2)*Y(2)
   F(4)=Y(5)
   F(5)=Y(6)
   F(6)=-0.5D0*Y(4)*Y(3)-0.5D0*Y(6)*Y(1)-X*R*Y(2)*Y(5)
   GO TO 30
20 A=1.0D0+(4.0D0/(3.0D0*CR))
   B=(PR*PSI)/2.0D0
   F(7)=Y(8)
   F(8)=-(B/A)*Y(8)
   F(9)=Y(10)
   F(10)=-(B/A)*Y(10)
30 RETURN
   END
```

VITA

Isaac W. Diggs was born in Sedley, Virginia, on July 18, 1949. He attended elementary schools in Southampton County, Virginia, and was graduated with honors from Riverview High School in June 1967. In September 1967 he entered Virginia State College where he became one of that institution's first Cooperative Education Program participants. This co-op experience culminated with publication of research he conducted and his designation as a Presidential Scholar by the Electron Microscopy Society of America.

Coincident with award of his Bachelor of Science degree in Physics in December 1971, the author was named Distinguished Military Graduate from the Advanced Army ROTC program and commissioned into the regular Army. During his seven years of active duty, his many assignments included a tour in Europe with a German Air Force missile unit, appointment to the faculty of the U.S. Army Air Defense School at Fort Bliss, Texas, and work as a prototype missile systems test officer at White Sands Missile Range, New Mexico. Upon his discharge from the Army in September 1978, he returned to work as a physicist with the Goodyear Atomic Corporation of Piketon, Ohio, where he had earlier completed his cooperative work experience. He was sent on extended assignment to Oak Ridge, Tennessee, as part of the Goodyear contingent working on the Gas Centrifuge Enrichment Plant Project for the U.S. Department of Energy.

Shortly after his assignment to Oak Ridge in 1978, the author entered the Graduate School of The University of Tennessee, Knoxville. He received the Master of Science degree with a major in Engineering Science in December 1980. Mr. Diggs will continue his employment with Goodyear Atomic Corporation after graduation.

The author is married to the former Chauncey Hazel of Petersburg, Virginia, and they have two sons, Isaac Jr., and Adam.